

Theoretical Performance Analysis of Vehicular Broadcast Communications at Intersection and their Optimization

Tatsuaki Kimura and Hiroshi Saito

Abstract—Cooperative vehicle safety (CVS) systems are a key application of intelligent transportation systems. In CVS systems, vehicles periodically broadcast their information, e.g., position, speed, and braking status. In this paper, we theoretically analyze the performance of vehicle-to-vehicle (V2V) broadcast communications at an intersection and provide tractable formulae of performance metrics to optimize them. We consider a model in which locations of vehicles are modeled separately as *queueing* and *running* segments and derive key performance metrics of V2V broadcast communications via a stochastic geometry approach. However, these theoretical expressions are highly complex and mathematically intractable, so we developed *closed-form* approximate formulae for them. In our approximation, the probability of successful transmission decreases geometrically as the distance to a receiver increases and is expressed by only system parameters. Using the approximate formulae, we propose a method for optimizing the broadcast rate of vehicles such that the mean number of successful receivers per unit time is maximized. Because of the closed form approximation, the optimal rate can be used as a guideline for a *real-time* control-method, which is not achieved through time-consuming simulations. We evaluated our approximation and optimization method through simulations and numerical experiments and found that the approximate formulae fitted well to exact analysis in a realistic setting. We also demonstrated the effectiveness of optimizing the broadcast rate.

I. INTRODUCTION

Intelligent transportation systems (ITSs) are promising technology for improving drivers/pedestrians safety and the efficiency of transportation [1]. In general, vehicle-to-infrastructure (V2I) and vehicle-to-vehicle (V2V) communications play a key role in achieving ITSs. These communications are commonly based on narrow-band dedicated short range protocols (DSRC). For instance, wireless access in vehicular environments (WAVE) is the protocol suite adopted in the U.S. In WAVE, IEEE 802.11p [2] is standardized for the media access control (MAC) and physical layers, and it uses 5.9-GHz bandwidth and carrier sense multiple access (CSMA) similar to IEEE 802.11a. In addition, IEEE 1609 [3] designs higher-layer functions such as networking and multichannel operations.

T. Kimura and H. Saito are with NTT Network Technology Laboratories, NTT Corporation, Tokyo 180-8585, Japan (e-mail: kimura.tatsuaki@lab.ntt.co.jp)

This work has been submitted to the IEEE for possible publication.

© 2017 IEEE. Personal use of this material is permitted. Permission from IEEE must be obtained for all other uses, in any current or future media, including reprinting/republishing this material for advertising or promotional purposes, creating new collective works, for resale or redistribution to servers or lists, or reuse of any copyrighted component of this work in other works.

Cooperative vehicle safety (CVS) systems [4] can be considered as one of the key applications of ITSs. CVS systems, working on DSRC protocols, include many applications such as cooperative collision warning, electronic emergency brake lights, and slow/stopped vehicle alerts [5]. In these systems, vehicles periodically broadcast their information e.g., car positions (Global Positioning System; GPS), speed, braking status, traffic status, and emergency information. By exchanging the information, vehicles can track the positions of other vehicles and avoid traffic congestion, collisions, or unknown hazards. CVS systems has been attracting much attention in recent decades because their rich applications will drastically change our lives.

Because of the critical nature of CVS systems, their performance analysis and management are hot research topics. Broadcasting with a high transmit power and high broadcast rate in congested roadways may significantly degrade the wireless communication quality due to high interference. To reduce the interference caused by a large number of vehicles sharing the same channel, several adaptive control schemes of the transmission power or broadcasting rate have recently been proposed [5], [6], [7], [8], [9], [10]. However, most of these schemes are not based on *theoretical* analysis and are commonly evaluated through simulations. Because the environments in which V2V communications occur may quickly and frequently change, a more general understanding of performance is crucial for the effective control of CVS systems. Furthermore, most studies consider only *homogeneous* environments, such as multi-lane highways, in which vehicles are running in the same direction with the same traffic density. However, to deploy CVS systems in urban environments in the future, more realistic *inhomogeneous* situations, such as intersections, must be taken into account. Most recently, a theoretical analysis was studied toward an optimization of transmission power of vehicles at an intersection [11]. However, the obtained analytical results are highly complicated and mathematically intractable, and thus the analysis cannot be applied to real-time control due to its high computational time.

In this paper, we perform theoretical analysis of V2V broadcast communications at an intersection and derive performance metrics in a tractable form. By expressing key performance metrics as *closed-form* approximate formulae, we can optimize the broadcast rate in a reasonable computational time so that the number of successful receivers per unit time is maximized. We consider an intersection model, in which locations of

vehicles are separated into *queueing* segments and *running* segments. In the former segment, vehicles are assumed to be queueing, i.e., stopped, at even intervals; and in the latter, vehicles are distributed in accordance with a homogeneous Poisson point process (PPP). By using a stochastic geometry approach, theoretical values of the key performance metrics of V2V broadcast communications are obtained: *the probability of successful transmission* and *the mean number of successful receivers*. The former is defined as the probability that the signal-to-interference-ratio (SIR) of a receiver exceeds a certain threshold, and the latter as the expected number of vehicles that can successfully receive information from a transmitter. However, these results from exact analysis are expressed in *non-analytical* form and need numerical integrals and multi-level summations for computing. Thus, they are too complicated not only to understand the forms of the function but also to optimize their system parameters due to large computational time. To address this problem, we developed a closed-form approximation for the performance metrics of V2V broadcast communications. More precisely, when vehicles broadcast to their neighbors, the probability of successful transmission geometrically decreases as the distance to the receiver increases in our approximation. In addition, the decay rate depends only on a few system parameters, such as the density of vehicles. Using the approximate formulae, we propose a method for optimizing the broadcast rate of vehicles that maximizes the number of successful receivers per unit time. By using the closed-form expression, we can easily compute the optimal broadcast rate without time-consuming numerical computation. Therefore, our optimization method can be applied to *real-time* broadcast rate control for CVS systems to mitigate the interference problem caused by congestion. Numerical experiments revealed our approximation fitted well to both simulation and exact analysis in a realistic setting. We also found that the proposed optimization could improve the interference problem at an intersection.

We briefly summarize our contributions as follows.

- We developed a closed-form approximation for the theoretical values of two key performance metrics of the performance of V2V broadcast communications at an intersection: the probability of successful transmission and the mean number of successful receivers. The approximate formulae depend only on system parameters and thus do not require time-consuming numerical computation.
- By using the approximation formulae, we developed a method for optimizing the broadcast rate of vehicles. Balancing the broadcast rate and the mean number of successful receivers, we improved V2V broadcast communications at a congested intersection. In accordance with the closed-form formulae, the optimal broadcast rate can be obtained in a reasonable computational time and thus can be applied to real-time broadcast rate control.
- We evaluated our approximation and optimization methods through simulation and numerical experiments. We found that our optimization method had sufficient performance. We also found that our approximation fitted well to the results from simulation and exact analysis in

a realistic setting.

The remainder of this paper is organized as follows. Section II summarizes previous studies. In Section III, we explain the proposed model considered in this paper. Section IV presents the main results of this paper, the approximate analysis of the key performance metrics of V2V communications at an intersection. In Section V, we explain a broadcast-rate-optimization method based on the analytical results. Finally, we discuss several numerical experiments in Section VI, and conclude the paper in Section VII.

II. RELATED WORK

Due to the importance of ITSs, there have been a lot of studies in the area of the performance evaluation of V2I/V2V communications in the past decade. Most of the earlier work is simulation-based [9], [12], [13], [14]. However, simulation-based approaches often require much computational time and resources. The previous work [15], [16], [17], [18] conducted a theoretical analysis of the CSMA behaviors of IEEE 802.11p on the basis of a Markov chain model approach. Fallah et al. [15] studied the impact of the rate and range of broadcasting on network performance in a highway environment considering the hidden terminal problem. Han et al. [17] and Yao et al. [18] analyzed the enhanced distributed channel access (EDCA) behavior in IEEE 802.11p, in which different access categories have different contention windows and arbitration inter-frame space. However, these studies did not consider the geographical effects or interference in V2V communications and assumed only simple communication scenarios.

To reduce the interference of V2V broadcast communications, several adaptive control schemes for transmission power [5], [9], [10] or broadcasting rate [5], [6], [7], [8] have recently been proposed. The method proposed by Moreno et al. [9] adaptively controls the transmission power of vehicles so that their max-min fairness is satisfied. In [10], a segment-based power control method based on a distributed vehicle density estimation algorithm is proposed. Huang et al. [5] developed broadcast rate and power control algorithms, in which the rate is determined by estimating the channel error rate and the power is determined by observing the channel status. Tielert et al. [8] introduced a rate adaptation algorithm based on the channel busy ratio. Most recently, Fallah et al. [7] updated the algorithm of [6] so that the power changes in each iteration can be configurable and stable. None of the adaptive control methods above was based on theoretical interference analysis and were considered in simple environments such as multi-lane highways, in which vehicles are running in the same direction with the same traffic density. However, theoretical guidelines for more realistic situations, such as intersections, are crucial to deploy CVS systems in more complex urban environments.

Stochastic geometry is a powerful mathematical tool for modeling random spatial events [19] and has recently been applied to the area of wireless communication [20], [21] including vehicular ad-hoc networks (VANET) [22], [23], [24], [25]. By modeling the locations of communication devices, such as vehicles and road side units (RSUs), as a spatial point process, theoretical values of various performance metrics can

be calculated. Such mathematical understanding of the ITS system not only frees us from time consuming simulation but also helps in optimization or sensitivity analysis of system parameters. In previous studies [24], [25], the behavior of CSMA used in DSRC was analyzed. More specifically, Nguyen et al. [24] showed that CSMA behaves like an ALOHA-type transmission pattern in dense networks and derived the theoretical expression of performance metrics in broadcast V2V communications while assuming that vehicles are distributed in accordance with spatially homogeneous PPP. In [25], the performance of DSRC in both the spatial and time domains was studied by using a Markov chain model approach for CSMA, which is similar to that of Nguyen et al. [26]. However, these studies focused on MAC behaviors of DSRC, considered only simple situations and did not take into account the impacts of heterogeneous urban structures, such as intersections.

III. MODEL DESCRIPTION

In this section, we explain the system model. Figure 1 shows a conceptual image of our model. We consider an intersection where two streets are crossing. One of the streets runs parallel along the x -axis, and the other along the y -axis. On the street along the x -axis, there are vehicles queueing, i.e., stopped, at the intersection, and on each street, vehicles are running. We call these parts a queueing segment S_Q or a running segment S_R . In addition, S_{R_x} and S_{R_y} denote the running segments on the x - or y -axis, respectively, i.e., $S_R = S_{R_x} \cup S_{R_y}$. We assume that vehicles in S_R are distributed in accordance with a homogeneous PPP on each street. Let λ_x and λ_y [1/km] denote the intensity of vehicles in S_{R_x} and S_{R_y} . Let n_+ and n_- denote the numbers of vehicles stopped at an intersection in each part, where the subscript $\{+,-\}$ represents the positive or negative direction on the x -axis. We assume that vehicles have length l_v and the widths of the streets are negligible. Note that there is no queue on the y -axis because we consider the case where the traffic signals on the y -axis are green. We can easily apply the same discussion in this paper to the case where those on the x -axis are green.

We next explain the channel model considered in this paper. Vehicles *periodically* broadcast radio signals, such as GPS, their braking information, or emergency information to neighbors, i.e., V2V communications. All vehicles are assumed to be equipped with devices necessary for V2V communications. We assume that each vehicle requires L [sec.] for each transmission and vehicles in S_Q independently transmit with rate $\theta \in (0, 1/L)$ [Hz] and those in S_R with $\theta_0 \in (0, 1/L)$. Thus, the probability that each vehicle in S_Q (resp. in S_R) is transmitting is equal to $\rho \triangleq \theta L \in (0, 1)$ [resp. $\rho_0 \triangleq \theta_0 L \in (0, 1)$]. We also assume that vehicles currently transmitting cannot simultaneously receive information from other vehicles. The transmission power of each vehicle is assumed to be equal to $1/\mu$ and constant. Antenna gain is assumed to be equal to 1 throughout this paper. All transmission channels have the effect of Rayleigh fading the random variable of which is denoted as h_i for vehicle i . The path loss model is $r^{-\alpha}$ for distance $r \in \mathbb{R}_+$, where $\alpha > 2$ is a path

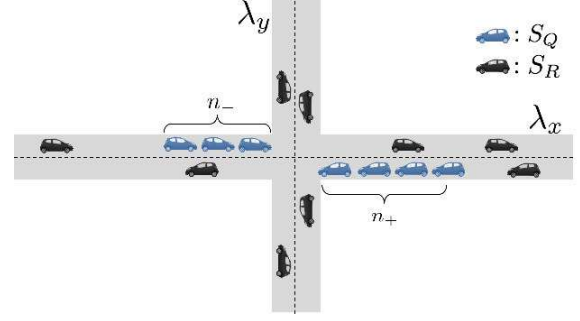


Fig. 1. System model. Vehicles in running segment (S_R) are distributed in accordance with homogeneous PPP with intensity λ_x or λ_y . Intervals of vehicles in queueing segment (S_Q) are fixed value l_v . n_+ and n_- represent number of vehicles stopping at intersection.

loss exponent. Thus, for instance, the received power from vehicle x_i at distance r can be expressed as $h_i r^{-\alpha} / \mu$. Table I summarizes the notations used in this paper.

TABLE I
LIST OF NOTATIONS

l_v	length of vehicle
S_R	set of vehicles running on street
S_{R_x}	set of vehicles running on street along x -axis
S_{R_y}	set of vehicles running on street along y -axis
S_Q	set of vehicles stopping/queueing at intersection
L	each transmission time
θ, θ_0	broadcast rate of vehicles in S_Q and S_R
ρ, ρ_0	probability that vehicles in S_Q and S_R are transmitting
λ_z	intensity of vehicles in S_R ($z \in \{x, y\}$)
n_*	number of vehicles stopped at intersection ($*$ $\in \{+, -\}$)
$1/\mu$	transmission power of vehicles in S_R
h_i	fading variable
I_R	interference from vehicles in S_{R_x}
I_Q	interference from vehicles in S_Q

Note that CSMA is designed as the MAC layer protocol in IEEE 802.11p [27]. Since vehicles that are close to each other do not transmit simultaneously in CSMA, hard-core point processes have been used for modeling such CSMA-based protocols [25], [26], [28]; however, they are not mathematically tractable because they are obtained by *dependent* thinning of a PPP. In addition, Nguyen et al. [24] claimed that CSMA behaves like an ALOHA-type transmission pattern in dense networks. Therefore, in this paper, we assume that transmitting vehicles use the ALOHA-type MAC protocol and follow a PPP because we focus on the congestion at the intersection and maintain the mathematical tractability.

Let I denote a random variable representing the total received power, i.e., interference power, from all the vehicles. If we consider the target channel in which the communication distance is equal to r , the SIR can be written as

$$\text{SIR}_r = \frac{h r^{-\alpha}}{\mu I}.$$

We then define the probability of successful transmission as the probability that the SIR of the target receiver exceeds a

threshold T , i.e.,

$$\begin{aligned} p(r) &\triangleq \mathbb{P}(\text{SIR}_r > T) = \mathbb{P}\left(\frac{hr^{-\alpha}}{\mu I} > T\right) \\ &= \mathbb{E}[\exp(-\mu Tr^\alpha I)] = \mathcal{L}_I(\mu Tr^\alpha), \end{aligned} \quad (1)$$

where $\mathcal{L}_I(s)$ is the Laplace transform of I . Probability $p(r)$ is a key performance metric of V2V broadcast communications, and thus, we mainly focus on the analysis of this value in our paper.

A. Performance Metrics

In this section, we provide theoretical expressions of performance metrics of V2V communications via a stochastic geometry approach. Since equation (1) shows that $p(r)$ can be obtained as the Laplace transform of the interference from vehicles, we first consider the interference distribution and then provide the theoretical values of the probability of successful transmission.

1) *Interference distribution*: We first consider the interference from vehicles in S_Q . For this purpose, we assume that the target receiver is in the positive part on the x -axis and at distance d from the intersection. In addition, let $d_m = |d - ml_v|$ ($1 \leq m \leq n_- + n_+$) denote the distance between the target receiver and the m -th vehicle from the intersection. We then have the following total interference power received from S_Q .

$$I_Q \triangleq \sum_{m=1}^{n_- + n_+} h_m \delta_m d_m^{-\alpha} / \mu,$$

where $\delta_m = 1$ if the m -th vehicle transmits, and $\delta_m = 0$ otherwise. Note that h_m is exponential with mean 1 according to the Rayleigh fading assumption. Note also that the vehicles in the S_Q are transmitting with the probability ρ . Therefore, the Laplace transform of I_Q can be obtained as

$$\begin{aligned} \mathcal{L}_{I_Q}(s | d) &\triangleq \mathbb{E}[\exp(-I_Q) | d] \\ &= \mathbb{E}\left[\exp\left(-\sum_{m=1}^{n_- + n_+} h_m \delta_m d_m^{-\alpha} / \mu\right)\right] \\ &= \prod_{m=1}^{n_- + n_+} \left[\frac{\mu \rho}{\mu + \frac{s}{(d_m)^\alpha}} + 1 - \rho \right]. \end{aligned} \quad (2)$$

We next consider the interference from the vehicles in S_R . Similar to the previous case, we assume that the target receiver is at distance d from the intersection in the positive part on the x -axis. Let Φ_R^X and Φ_R^Y denote PPPs corresponding to S_{R_x} and S_{R_y} . The total interference from Φ_R^X can be represented as $I_R^X = \sum_{x_i \in \Phi_R^X} h_i |x_i - d|^{-\alpha} / \mu$. Recall that vehicles in S_R transmit with probability ρ_0 . By following a well-known computation of the Laplace functional of the Poisson point process (see e.g., Proposition 1.5 and Corollary 2.9 in [29]), we can compute the Laplace transform of I_R^X as follows.

$$\begin{aligned} \mathcal{L}_{I_R^X}(s) &\triangleq \mathbb{E}\left[\exp\left(-s \sum_{x_i \in \Phi_R^X} \frac{h_i}{\mu |x_i - d|^\alpha}\right)\right] \\ &= \exp\left(-\rho_0 \lambda_x \int_{-\infty}^{\infty} \frac{s}{\mu |x|^\alpha + s} dx\right). \end{aligned} \quad (3)$$

Note that the distance from the tagged vehicle to a vehicle at distance y from the intersection on the y -axis is equal to $\sqrt{y^2 + d^2}$. Thus, if I_R^Y denotes the total interference from Φ_R^Y , we have $I_R^Y = \sum_{y_i \in \Phi_R^Y} h_i (y_i^2 + d^2)^{-\alpha/2} / \mu$. Therefore, similar to (3), we obtain (see also Section 2 in [11]),

$$\begin{aligned} \mathcal{L}_{I_R^Y}(s | d) &\triangleq \mathbb{E}\left[\exp\left(-s \sum_{y_i \in \Phi_R^Y} \frac{h_i}{\mu (y_i^2 + d^2)^{\frac{\alpha}{2}}}\right)\right] \\ &= \exp\left(-\rho_0 \lambda_y \int_{-\infty}^{\infty} \frac{s}{\mu (y^2 + d^2)^{\frac{\alpha}{2}} + s} dy\right). \end{aligned} \quad (4)$$

2) *Probability of successful transmission*: Note that the Laplace transform of the total interference from all the vehicles can be represented as

$$\begin{aligned} \mathcal{L}_I(s) &= \mathbb{E}[\exp(-sI)] = \mathbb{E}[\exp(-s(I_Q + I_R^X + I_R^Y))] \\ &= \mathcal{L}_{I_Q}(s | d) \mathcal{L}_{I_R^X}(s) \mathcal{L}_{I_R^Y}(s | d), \end{aligned}$$

where $\mathcal{L}_{I_Q}(s | d)$, $\mathcal{L}_{I_R^X}(s)$, and $\mathcal{L}_{I_R^Y}(s | d)$ are given in (2)–(4), respectively. Thus, by applying this to (1), we can easily obtain the probability of successful transmission as follows.

Proposition III.1 *Suppose that the target transmitter is at distance $d \geq 0$ from an intersection. The probability of successful transmission to a vehicle at distance $r > 0$ from the transmitter on the x -axis is equal to*

$$p(r) = \mathcal{L}_{I_Q}(\mu Tr^\alpha | d') \mathcal{L}_{I_R^X}(\mu Tr^\alpha) \mathcal{L}_{I_R^Y}(\mu Tr^\alpha | d'), \quad (5)$$

where $d' = d + r$ if the receiver is on the right-hand side of the transmitter, and $d' = |d - r|$ otherwise.

3) *Mean number of successful receivers*: Using Proposition III.1, we can also obtain the mean number of successful receivers, which is defined as the expected number of vehicles to which the target transmitter can transmit. This metric can be considered as a key performance metric of V2V broadcast communications and is also considered in [24] under a homogeneous PPP environment. Note that there are three types of receivers: vehicles in S_Q , in S_{R_x} , and in S_{R_y} . Recall also that vehicles transmitting radio waves cannot simultaneously receive information from other vehicles. From these facts, we obtain the following result.

Proposition III.2 *If the target transmitter is the d -th vehicle from an intersection, the mean number of successful receivers \bar{M} is given by*

$$\begin{aligned} \bar{M} &= (1 - \rho) \sum_{i=-n_-, i \neq d}^{n_+} p(|d - i|l_v) \\ &+ (1 - \rho_0) \left[\lambda_x \int_{\mathbb{R}} p(r) dr + \lambda_y \int_{\mathbb{R}} p(\sqrt{(dl_v)^2 + r^2}) dr \right]. \end{aligned} \quad (6)$$

IV. APPROXIMATE FORMULAE OF PERFORMANCE METRICS

Although theoretical values of the performance metrics can be obtained as in Propositions III.1 and III.2, they are expressed in non-analytical forms [see (2)–(6)]. Therefore, it is difficult not only to see the impacts of various parameters

on them but also to optimize their system parameters because numerical integrals and multi-level summations are included. Thus, if we apply any numerical optimization methods to obtain optimal system parameters, a large computational time is required because of these heavy computations in each step of the numerical methods. To solve this problem, we attempt to obtain a closed-form approximation for $p(r)$ and \bar{M} that depends only on system parameters. We then propose an optimization method for the broadcast rate of vehicles in S_Q (see Section V). In accordance with the closed-form approximation, we can solve the optimization problem in a reasonable computational time, and thus, it can be applied to real-time broadcast rate control for CVS systems.

In general, the characteristics of $p(r)$ and \bar{M} depend on the location of the target transmitter. To obtain closed-form formulae, we consider three typical locations of the target transmitter instead of considering arbitrary locations of the transmitter: the target transmitter is in the positive direction on the x -axis and (A) at the intersection, (B) at the end of the queue, and (C) in the middle of the queue (see Figure 2). Since a vehicle at (or near) the intersection is affected by interferences from both directions (x - and y -axis directions) and queues, the vehicle is expected to have the worst performance, and its performance can be approximated by case (A). A vehicle at (or near) the end of the queue is said to be in an intermediate state of vehicles between the queueing and running segments. Thus, we approximate it by considering case (B). The performance in this case can characterize the traffic heterogeneity at the intersection. In case (C), the transmitter is far from both the end of the queue and the street along the y -axis. Thus, if the queue is sufficiently long, the performance in this case can be approximated as vehicles stopping at even intervals on a 1-d line with infinite length.

Note that the performance of vehicles at other positions can be estimated by interpolating or extrapolating those in cases (A)–(C) (detailed discussion is given in Section VI-C). Note also that if a vehicle is in S_{R_x} and far from the end of the queue, its performance can be estimated by considering vehicles homogeneously distributed on a 1-d line, i.e., the effect of queues is negligible. Thus, we do not consider this simple case in this paper. In addition, we can consider the case where the transmitter is in S_{R_y} by combining case (A) and a model with a single street. Therefore, we analyze cases (A)–(C) because they characterize the effect of the intersection.

As we can see later, we can calculate the analytical values of $\mathcal{L}_{I_R^X}(\mu Tr^\alpha)$ and $\mathcal{L}_{I_R^Y}(\mu Tr^\alpha)$ in special cases, such as $\alpha \in \mathbb{N}$. However, the term $\mathcal{L}_{I_Q}(\mu Tr^\alpha)$, i.e., the interference from S_Q , cannot be expressed in an analytical form even in such cases. Therefore, we mainly focus on giving a closed-form approximation for $\mathcal{L}_{I_Q}(\mu Tr^\alpha)$ in this paper. The obtained approximate formulae for $\mathcal{L}_{I_Q}(\mu Tr^\alpha)$ basically hold under conditions in which $\alpha \in \mathbb{N}$ and queue lengths n_+ and n_- are sufficiently large.

A. Case (A): Transmitter at Intersection

We first consider case (A), where the transmitter is at an intersection. As mentioned in Section III-A3, there are three types of receivers: a receiver in S_Q , in S_{R_x} , and in S_{R_y} .

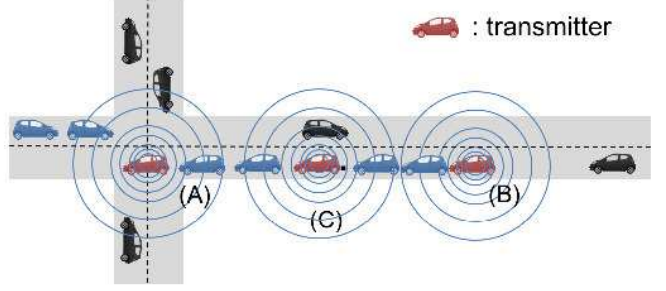


Fig. 2. Three typical cases considered in Section IV: (A) target transmitter is at intersection, (B) at end of queue, and (C) in middle of queue.

1) *Probability of successful transmission:* We first provide approximation for the probability of successful transmission when transmitting to a receiver in S_Q . Note that if a receiver is in S_Q and the i -th vehicle from the intersection, the communication distance is equal to il_v . Detailed explanation for the derivation of the formulae below is given in Appendix A-A.

Approximate formulae of $p(r)$ in case (A): Suppose that the transmitter is at an intersection. If $(1 - \rho)T \geq 1^1$ and $\alpha \in \mathbb{N}$, the probability of successful transmission can be approximated as follows. (i) If a receiver is the i -th vehicle from an intersection, then

$$p(il_v) \approx \frac{1 + T}{(1 - \rho)(1 + (1 - \rho)T)} \times \exp \left[\left(2\xi_{\alpha,T}(\rho) - \pi\rho_0 (\lambda_x C_{\alpha,T}^X + \lambda_y C_{\alpha,T}^Y) l_v \right) i \right], \quad (7)$$

where, for $\alpha \in \mathbb{N}$,

$$\xi_{\alpha,T}(\rho) = (\alpha + \kappa_{1,\alpha} - \kappa_{2,\alpha})((1 - \rho)^{1/\alpha} - 1)T^{1/\alpha}, \quad (8)$$

$$\kappa_{1,\alpha} = \alpha \sum_{k=1}^{\infty} \frac{(-1)^{k+1}}{ak - 1}, \quad \kappa_{2,\alpha} = \alpha \sum_{k=1}^{\infty} \frac{(-1)^{k+1}}{ak + 1}, \quad (9)$$

and

$$C_{\alpha,T}^X = T^{\frac{1}{\alpha}} \int_{-\infty}^{\infty} \frac{dx}{x^\alpha + 1}, \quad C_{\alpha,T}^Y = T \int_{-\infty}^{\infty} \frac{dy}{(y^2 + 1)^{\frac{\alpha}{2}} + T}, \quad (10)$$

(ii) if a receiver is in S_{R_x} at distance $r > 0$ from the intersection, then

$$p(r) \approx \frac{1 + T}{1 + (1 - \rho)T} \times \exp \left[\left(\frac{2\xi_{\alpha,T}(\rho)}{l_v} - \pi\rho_0 (\lambda_x C_{\alpha,T}^X + \lambda_y C_{\alpha,T}^Y) \right) r \right], \quad (11)$$

and (iii) if a receiver is in S_{R_y} at distance $r > 0$ from the intersection, then

$$p(r) \approx \frac{1}{(1 - \rho)^{2r}} \frac{1 + T}{1 + (1 - \rho)T} \cdot \exp \left[\left(\frac{2\xi_{\alpha,T}(\rho)}{l_v} - \frac{2\rho}{(\alpha + 1)(1 - \rho)Tl_v} - \pi\rho_0 (\lambda_x C_{\alpha,T}^X + \lambda_y C_{\alpha,T}^Y) \right) r \right]. \quad (12)$$

¹A typical value of the outage threshold T is 10–15 dB (for example, 10 ~ 15 dB ($\approx 10 \sim 35.63$) in IEEE 802.11p). In addition, the optimal ρ was often less than 0.4 in our experiments. Thus, this assumption can be considered as valid. In addition, we can also derive an approximate formula for other cases using the results in Appendix A.

Remark IV.1 $\kappa_{1,\alpha}$ and $\kappa_{2,\alpha}$ in (9) and $C_{\alpha,T}^X$ and $C_{\alpha,T}^Y$ in (10) depend only on α and T , and thus they can be determined in accordance with the communication environment. In addition, $C_{\alpha,T}^X$ and $C_{\alpha,T}^Y$ in (10) are expressed as integral forms, but, they can be computed analytically in some spacial cases, such as $\alpha = 2, 4$. For example,

$$C_{\alpha,T}^X = \frac{\pi}{\alpha} \csc\left(\frac{\pi}{\alpha}\right), \quad \alpha \in \mathbb{N},$$

$$C_{\alpha,T}^Y = \begin{cases} \frac{\sqrt{T}\sqrt{\sqrt{1+T}-1}}{2\sqrt{1+T}}, & \alpha = 4, \\ \frac{T}{\sqrt{1+T}}, & \alpha = 2. \end{cases}$$

The approximate formulae (7), (11), and (12) suggest that, in our approximation, the probability of successful transmission decreases geometrically with the distance to receivers. For example, if a receiver is in S_Q , then the geometric decay rate is equal to

$$\exp(2\xi_{\alpha,T}(\rho) - \pi\rho_0(\lambda_x C_{\alpha,T}^X + \lambda_y C_{\alpha,T}^Y)l_v),$$

which is determined by only system parameters and can be easily computed using (8)–(10). The same applies to the case where a receiver is in S_{R_x} or S_{R_y} .

2) *Mean number of successful receivers:* From the results in the previous section, we can approximate the mean number of successful receivers. Since the approximate formulae of $p(r)$ are expressed in a geometric form, we can also obtain a closed-form approximation for \overline{M} . Let $\overline{M}_Q(\rho)$, $\overline{M}_{R_X}(\rho)$, and $\overline{M}_{R_Y}(\rho)$ denote the mean numbers of successful receivers in S_Q , S_{R_x} , and S_{R_y} , respectively. First, applying (7) to Proposition III.2 and considering sufficiently large n_+ and n_- , we obtain

$$\overline{M}_Q(\rho) \approx 2(1-\rho) \sum_{i=1}^{\infty} p(il_v) \approx \frac{1+T}{1+(1-\rho)T} \times \frac{2\rho \exp(2\xi_{\alpha,T}(\rho) - \pi\rho_0(\lambda_x C_{\alpha,T}^X + \lambda_y C_{\alpha,T}^Y)l_v)}{1 - \exp(2\xi_{\alpha,T}(\rho) - \pi\rho_0(\lambda_x C_{\alpha,T}^X + \lambda_y C_{\alpha,T}^Y)l_v)}, \quad (13)$$

Similar to the above, from (11) and (12), we can approximate $\overline{M}_{R_X}(\rho)$ and $\overline{M}_{R_Y}(\rho)$ as follows.

$$\overline{M}_{R_X}(\rho) = 2(1-\rho_0)\lambda_x \int_{r=0}^{\infty} p(r)dr \approx \frac{1+T}{1+(1-\rho)T} \frac{2(1-\rho_0)\lambda_x l_v}{2\xi_{\alpha,T}(\rho) - \pi\rho_0(\lambda_x C_{\alpha,T}^X + \lambda_y C_{\alpha,T}^Y)l_v}. \quad (14)$$

$$\overline{M}_{R_Y}(\rho) = 2(1-\rho_0)\lambda_y \int_{r=0}^{\infty} p(r)dr \approx 2(1-\rho_0)\lambda_y l_v \left(\frac{1+T}{1+(1-\rho)T} \right) [2\xi_{\alpha,T}(\rho) - 2\log(1-\rho) - \frac{2\rho}{(\alpha+1)(1-\rho)T} - \pi\rho_0(\lambda_x C_{\alpha,T}^X + \lambda_y C_{\alpha,T}^Y)l_v]^{-1}. \quad (15)$$

B. Case (B): Transmitter at End of Queue

We next consider case (B), where the transmitter is at the end of the queue. In this case, the transmitter is far from the y -axis due to the queueing segment. Therefore, the interferences

from the vehicles in S_{R_y} and the receivers in S_{R_y} are both negligible. This case can be divided into three sub-cases: a receiver is in (i) S_Q , in (ii) S_{R_x} in the negative direction, or (iii) S_{R_x} in the positive direction, i.e., the left-hand side of the transmitter or the right-hand side (see Figure 2).

1) *Probability of successful transmission:* As mentioned above, the interference from the vehicles in S_{R_y} is relatively much smaller than that from S_Q and S_{R_x} regardless of the position of a receiver. Thus, the term $\mathcal{L}_{I_Y}(\mu Tr^\alpha)$ is negligible, i.e.,

$$p(r) \approx \mathcal{L}_{I_Q}(\mu Tr^\alpha) \mathcal{L}_{I_X^R}(\mu Tr^\alpha). \quad (16)$$

We then have the following results, in which $p(r)$ also decreases geometrically as r increases; however, the decay rate is different from that in case (A). Detailed explanation for the derivation of the formulae below is given in Appendix A-B.

Approximate formulae of $p(r)$ in case (B): Suppose that the transmitter is at the end of the queue and $(1-\rho)T \geq 1$. If $\alpha \in \mathbb{N}$, the probability of successful transmission can be approximated as follows. (i) If a receiver is in S_Q and the i -th vehicle from the end of the queue, then

$$p(il_v) \approx e^{\frac{\rho}{2(1-\rho)T}} (1-\rho)^{i-\frac{1}{2}} \frac{1+T}{1+(1-\rho)T} \times \exp[(\beta_{\alpha,T}(\rho) - \pi\rho_0\lambda_x C_{\alpha,T}^X l_v) i], \quad (17)$$

where

$$\beta_{\alpha,T}(\rho) = \xi_{\alpha,T}(\rho) + \frac{\rho}{(1-\rho)(\alpha+1)T}, \quad (18)$$

(ii) if a receiver is in S_{R_x} in the negative direction and at distance $r > 0$ from the end of the queue, then

$$p(r) \approx e^{\frac{\rho}{2(1-\rho)T}} (1-\rho)^{\frac{r}{l_v}+\frac{1}{2}} \frac{1+T}{1+(1-\rho)T} \times \exp\left[\left(\frac{\beta_{\alpha,T}(\rho)}{l_v} - \pi\rho_0\lambda_x C_{\alpha,T}^X\right) r\right], \quad (19)$$

and (iii) if a receiver is in S_{R_x} in the positive direction and at distance $r > 0$ from the end of the queue, then

$$p(r) \approx \sqrt{\frac{1+T}{1+(1-\rho)T}} (1-\rho)^{-\frac{r}{l_v}} \exp\left[\left(\frac{\xi_{\alpha,T}(\rho)}{l_v} - \frac{\rho}{(\alpha+1)(1-\rho)Tl_v} - \pi\rho_0\lambda_x C_{\alpha,T}^X\right) r\right]. \quad (20)$$

2) *Mean number of successful receivers:* Similar to case (A) considered in Section IV-A, the approximate formulae presented in Section IV-B1 are in geometric forms. This fact again enables us to obtain the closed-form approximation $\overline{M}(\rho)$. Recall here that $\overline{M}_{R_Y}(\rho)$ is negligible in this case due to the distance between the transmitter and the y -axis. Thus, by using (17), (19), (20), and Proposition III.2, we can approximate $\overline{M}_Q(\rho)$ and $\overline{M}_{R_X}(\rho)$ as

$$\overline{M}_Q(\rho) \approx \sqrt{1-\rho} \exp\left(\frac{\rho}{2(1-\rho)T}\right) \frac{1+T}{1+(1-\rho)T} \times \frac{\exp(\beta_{\alpha,T}(\rho) - \pi\rho_0\lambda_x C_{\alpha,T}^X l_v)}{1 - (1-\rho) \exp(\beta_{\alpha,T}(\rho) - \pi\rho_0\lambda_x C_{\alpha,T}^X l_v)}, \quad (21)$$

$$\begin{aligned}
\overline{M}_{R_X}(\rho) &\approx \sqrt{1-\rho} \exp\left(\frac{\rho}{2(1-\rho)T}\right) \frac{1+T}{1+(1-\rho)T} \\
&\times \frac{(1-\rho_0)\lambda_x l_v}{\beta_{\alpha,T}(\rho) + \log(1-\rho) - \pi\rho_0\lambda_x C_{\alpha,T}^X l_v} \\
&+ (1-\rho_0)\lambda_x l_v \sqrt{\frac{1+T}{1+(1-\rho)T}} [\xi_{\alpha,T}(\rho) \\
&- \log(1-\rho) - \frac{\rho}{(\alpha+1)(1-\rho)T} - \pi\rho_0\lambda_x C_{\alpha,T}^X l_v]^{-1}. \quad (22)
\end{aligned}$$

C. Case (C): Transmitter in Middle of Queue

Finally, we consider case (C), where the transmitter is in the middle of the queue.

1) *Probability of successful transmission:* As well as case (B), if the queue is sufficiently long, then we can neglect the interference from S_{R_y} and $\overline{M}_{R_Y}(\rho)$. Thus, we approximate this case by considering vehicles queuing at even intervals on a single street with infinite length, i.e., a single infinite queue. Under this assumption, we can obtain the approximate formulae for this case by simply removing the effect of the interference from vehicles on the y -axis in the results in Section IV-A1. Thus, substituting $\lambda_y = 0$ into (7) and (11), we can immediately obtain the following.

Approximate formulae of $p(r)$ in case (C): Suppose that the transmitter is in the middle of the queue. If $(1-\rho)T \geq 1$ and $\alpha \in \mathbb{N}$, the probability of successful transmission can be approximated as follows. (i) If a receiver is the i -th vehicle from the transmitter, then

$$\begin{aligned}
p(il_v) &\approx \frac{1+T}{(1-\rho)(1+(1-\rho)T)} \\
&\times \exp\left[\left(2\xi_{\alpha,T}(\rho) - \pi\rho_0\lambda_x C_{\alpha,T}^X l_v\right) i\right], \quad (23)
\end{aligned}$$

and (ii) if a receiver is in S_{R_x} at distance r from the intersection, then

$$p(r) \approx \frac{1+T}{1+(1-\rho)T} \exp\left[\left(\frac{2\xi_{\alpha,T}(\rho)}{l_v} - \pi\rho_0\lambda_x C_{\alpha,T}^X\right) r\right]. \quad (24)$$

2) *Mean number of successful receivers:* As mentioned in the above, the number of the successful receivers in S_{R_y} is relatively small in this case. Therefore, it is sufficient to consider receivers in S_Q and S_{R_x} . In a similar way to the derivation of (13), we also easily obtain an approximation for $\overline{M}_Q(\rho)$ and $\overline{M}_{R_X}(\rho)$ by substituting $\lambda_y = 0$ into (13) and (14), respectively.

$$\overline{M}_Q(\rho) \approx \frac{1+T}{1+(1-\rho)T} \frac{2\rho \exp(2\xi_{\alpha,T}(\rho) - \pi\rho_0\lambda_x C_{\alpha,T}^X l_v)}{1 - \exp(2\xi_{\alpha,T}(\rho) - \pi\rho_0\lambda_x C_{\alpha,T}^X l_v)}, \quad (25)$$

Similar to the above, from (11) and (12), we can approximate $\overline{M}_{R_X}(\rho)$ and $\overline{M}_{R_Y}(\rho)$ as follows.

$$\overline{M}_{R_X}(\rho) \approx \frac{1+T}{1+(1-\rho)T} \frac{2(1-\rho_0)\lambda_x l_v}{2\xi_{\alpha,T}(\rho) - \pi\rho_0\lambda_x C_{\alpha,T}^X l_v}. \quad (26)$$

V. BROADCAST RATE OPTIMIZATION

We next consider the optimization of the broadcast rate θ of vehicles in the S_Q on the basis of the approximate formulae of the performance metrics presented in Section IV. If the vehicles in S_Q transmit with a high broadcast rate, then they have higher interference than those in S_R due to the congestion of vehicles at the intersection. Therefore, the probability of successful transmission for the transmitter in S_Q becomes lower than that for the transmitter in S_R . However, there are more vehicles near the intersection than in S_R , and thus, the transmitter in S_Q has more vehicles to transmit. In addition, if a vehicle transmits with a high broadcast rate, it has more chance to successfully transmit to its neighbors. Thus, to characterize and balance this relationship, we consider the *mean number of successful transmissions per unit time*, which is equal to

$$D(\rho) = \rho \overline{M}(\rho). \quad (27)$$

Note here that we directly optimize the value ρ , not θ , because $\rho = \theta L$ and L is assumed to be constant. By using $D(\rho)$ as a cost function of ρ , we consider the optimization problem

$$\rho_* = \arg \max_{0 \leq \rho \leq 1} D(\rho). \quad (28)$$

By solving the above problem, we can obtain the optimal broadcast rate θ that maximizes the mean number of successful transmissions per unit time. In addition, by substituting the approximate formulae of $\overline{M}_Q(\rho)$, $\overline{M}_{R_X}(\rho)$, and $\overline{M}_{R_Y}(\rho)$ [shown in (13)–(15), (21), and (22)] with (27), we can consider the optimization problem of the broadcast rate in cases (A)–(C). In our experiments, we found that ρ_* in case (C) can roughly maximize $D(\rho)$ in cases (A) and (B) if the traffic intensity in S_R is not very high. Therefore, by applying this value to the broadcast rate of all the vehicles in S_Q , we can optimize the performance of broadcasting in all three cases (for details, see Section VI-B).

Since the values from exact analysis shown in Propositions III.1 and III.2 include numerical integrals and multi-level summations, the calculation of the exact value of $D(\rho)$ requires a large computational cost. Furthermore, its optimization becomes much more time-consuming because such a heavy computation is needed in each step of numerical optimization methods. However, by using the closed-form approximation of $D(\rho)$, we can compute the optimal ρ_* in a reasonable computational time. Because we found that $D(\rho)$ and $M(\rho)$ are mostly insensitive to n_+ and n_- , we adopted a long queue assumption in our approximation. As a result, if we assume that α , T , and ρ_0 are given in advance, ρ_* can be determined by only λ_x and λ_y . This fact suggests that if we prepare a look-up table in our vehicles that describes the optimal broadcast rate corresponding to each value of λ_x and λ_y , we can immediately optimize the broadcast rate by just obtaining the current traffic density in the running segments. This fact leads to the possibility of (near-)optimal real-time broadcast rate control. However, considering all possible cases for n_+ , n_- , λ_x , and λ_y is unrealistic for the exact analysis.

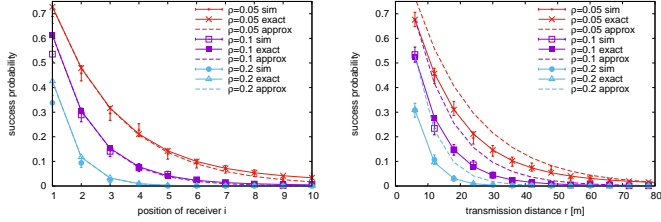


Fig. 3. Comparison of values of $p(r)$ in case (A) from simulation/exact/approximate analysis with different ρ when $N = 25$ and receiver is i -th vehicle from intersection in S_Q (left) and S_{R_y} (right).

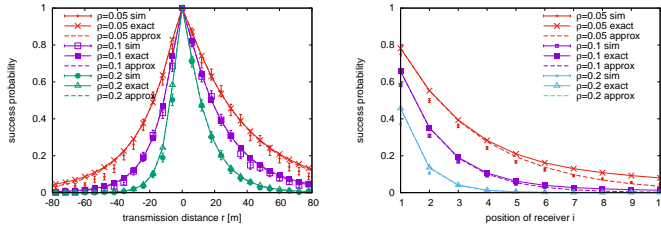


Fig. 4. Comparison of values of $p(r)$ in case (B) from simulation/exact/approximate analysis with different ρ when $N = 25$.

Fig. 5. Comparison of values of $p(r)$ in case (C) from simulation/exact/approximate analysis with different ρ when $N = 25$ and receiver is in S_Q and is i -th vehicle from transmitter.

VI. EXPERIMENTS

In this section, we provide the results from several numerical experiments. We first show the experimental results for the performance metrics $p(r)$ and $\overline{M}(\rho)$. We evaluate our approximate formulae in cases (A)–(C) considered in Sections IV-A–IV-C with both simulation and exact results. We then discuss our broadcast-rate optimization method presented in Section V. Finally, we investigate the performance of vehicles at other locations by interpolating or extrapolating the results for cases (A)–(C).

Before we move on to the experimental results, we will explain the parameters used in the experiments. The interval of vehicles l_v was fixed to 6 [m] and $\alpha = 4$ in all experiments. By considering realistic settings, we chose $\rho_0 = 0.1$ and $T = 15$ [dB]. In addition, $\lambda \triangleq \lambda_x = \lambda_y = 25$ [km^{-1}] and $n_+ = n_- = N$.

A. Evaluation of Performance Metrics

In this subsection, we provide the experimental results for the performance metrics $p(r)$ and $\overline{M}(\rho)$ and evaluate the accuracy of our approximate formulae for them. Figure 3 compares the simulation results and the exact and approximate values of $p(r)$ in case (A) i.e., the case where the transmitter is at the intersection (see Section IV-A). The left graph corresponds to the case where the receiver is in the S_Q and the i -th vehicle from the intersection. In addition, the right graph shows the case where the receiver is in S_{R_y} and the horizontal axis represents the transmission distance. All error-bars in the graphs in this paper represent 95% confidence intervals. We calculated the values from exact analysis using (5) and those from approximate analysis using (7) [left graph] and (12) [right graph]. We can see from the left graph that $p(r)$ geometrically

decreased, and if ρ increases $p(r)$ also decreases due to higher interference from vehicles in S_Q . We can also see that our approximate formula fit well to the results from simulation and exact analysis in all cases and the error became larger when i was larger. The reason for this can be considered as follows. Since we assume that N is sufficiently large in our approximation, if the distance from the receiver to the end of the queue is closer, then the approximation error becomes large. From the right graph, we can find that the approximate formulae took higher values than the theoretical results and the error increased subject to ρ . The reason for this is that we approximate the Euclidean distance from the receiver in S_{R_y} to the transmitter at the intersection by the Manhattan distance (see (40) in Appendix A-A). Thus, the interference became smaller and $p(r)$ became larger than in the simulation and exact analysis. In addition, the larger ρ suggests that there were greater impacts from the interference from the vehicles in S_Q . Therefore, the errors increased subject to ρ . Although the errors in the right graph were larger than those in the left one, we could obtain a rough estimation for $p(r)$. Indeed, we later determined that the errors could be negligible when considering $\overline{M}(\rho)$ (see Figure 6).

Similarly, Figure 4 shows the results of our approximation and the simulation and exact analysis for $p(r)$ in case (B) where the transmitter is at the end of the queue. The horizontal axis represents the distance to the receiver where the positive (resp. negative) part corresponds to the vehicles in the right-hand side, i.e., in S_{R_x} (resp. the left-hand side, i.e., in S_Q) of the transmitter. We used (5) for the exact analysis and (17) and (20) for the approximate one. Thus, we can see from the figure that if ρ is smaller, the results on the positive and negative parts become closer because the interference from the S_Q decreases. This is because the interference from the S_Q decreases as ρ decreases. The figure also shows that our approximate formula achieved quite small errors in all cases. Figure 5 shows the experimental results for case (C), where the transmitter is in the middle of the queue. The values of exact analysis in (5) were approximated by using (23). The figure shows a similar tendency to case (A) (see Figure 3) because the results can be computed very similarly.

We next show the results for $\overline{M}(\rho)$. Figure 6 compares the simulation results and the exact and approximate values of $\overline{M}(\rho)$. The left, middle, and right graphs correspond to cases (A), (B), and (C), respectively. The values from the exact analysis are calculated by (6) whereas those from the approximate analysis corresponding to cases (A), (B), and (C) are calculated by using (13)–(15), (21) and (22), and (25) and (26), respectively. We can see from the graphs that $\overline{M}(\rho)$ rapidly decreased as ρ increased. In addition, if N was larger, $\overline{M}(\rho)$ became smaller because the interference at the intersection became higher. We can also see that our approximation performed well except for region ρ , which was larger than 0.8 in case (A). Furthermore, the errors increased when N was small. Similar to the evaluation of $p(r)$, this is because we assume that the queue length N is sufficiently large in our approximation. However, the optimal ρ_* is usually around $0.05 \sim 0.2$ (see also Section VI-B), and thus, we regard our approximate formulae for $\overline{M}(\rho)$ as having sufficient

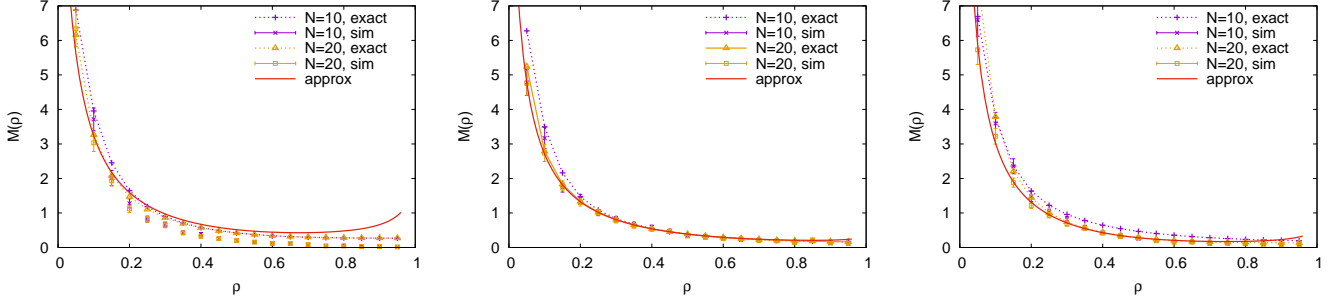


Fig. 6. Comparison of values of $\bar{M}(\rho)$ from simulation/exact/approximate analysis with different ρ and N . Left, middle, and right figures correspond to cases (A), (B), and (C).

accuracy in realistic settings. In addition, we can find that the errors in the graph in Figure 3 did not have much effect on the approximation for $\bar{M}(\rho)$.

B. Effectiveness of Optimization Method

In this subsection, we provide the evaluation results for the optimization method presented in Section V. Figure 7 shows the results for the cost function $D(\rho)$ with different ρ and N . We also plotted the optimal ρ_* 's that maximized the approximate $D(\rho)$ in the same graphs. The left, middle, and right graphs correspond to cases (A), (B), and (C), respectively. All values in the graphs were calculated by using (6) or approximate formulae in Section IV. We first focus on the results from the exact analysis. We can see from the graphs that there exist local maximum values in the domain $\rho \leq 0.5$ in all cases. The figure shows that the optimal ρ 's achieved roughly 10% higher $D(\rho)$ at the maximum. Furthermore, when ρ approached 1, $D(\rho)$ from the exact analysis slightly increased. This is because we fixed the broadcast rate θ_0 of the vehicles in S_R . Thus, if ρ increases, the transmitter has more of a chance to transmit to vehicles in S_R although the probability of successful transmission becomes smaller. However, ρ larger than 0.5 is unrealistic when considering a realistic receiving time and other computational time, e.g., encoding. Thus, we assume optimal ρ_* is in the domain $\rho \leq 0.5$. Indeed, in our experimental settings, we can see that unique optimal ρ_* 's exist in that domain.

We next discuss the accuracy of our approximation. We can see from the graphs that the values of $D(\rho)$ with our approximation fitted well to those from the exact analysis in the domain $\rho \leq 0.5$. We can also see that the value of ρ_* was not very sensitive to the value of N in all cases. This fact suggests that our approximate $D(\rho)$ not depending on N is valid. However, the errors between the values from the exact and approximate analysis became larger when N was smaller or ρ was larger. The reason for this is that, in our approximation, we assume that N is sufficiently large and $(1 - \rho)T > 1$. Thus, in the region where N is small or ρ is close to 1, the accuracy of the approximate formulae becomes worse. In addition, the errors in the left graph in the domain $\rho \geq 0.5$ were larger than those in the middle and right ones. The reason for this is that we approximated the Euclidean distance from the receiver in S_{R_y} to the vehicles in S_Q by the Manhattan distance, which is larger than the Euclidean one.

Thus, the interference from the vehicles in S_Q to the receivers in S_{R_y} was underestimated. Consequently, the approximate values of $D(\rho)$ were larger than those in the exact analysis. However, the errors are relatively small in the domain where the optimal ρ_* existed and $\rho \leq 0.5$. Therefore, we can say that the optimization with our approximation provides a good guideline for the optimal ρ_* .

We next discuss how we can determine the single optimal ρ_* for the vehicles in S_Q . Since our optimization problem depends on cases (A)–(C), we need to choose or derive a single ρ that can be optimal for the vehicles in the S_Q from these solutions. Figure 8 compares results of the values of $D(\rho_*)$ in all three cases with different λ . We also plotted $D(\rho_c)$ in cases (A) and (B) as the dashed and dotted lines, respectively, where ρ_c is equal to ρ_* in case (C). In addition, we fixed $N = 25$. We can see from the figure that $D(\rho_*)$ and $D(\rho_c)$ took similar values when λ was smaller than 40. This fact is supported by Fig. 7, in which $D(\rho)$ was insensitive to ρ around ρ_* . Therefore, by adopting ρ_c to determine the broadcast rate of all vehicles in S_Q , we can roughly maximize $D(\rho)$ in all the cases if the traffic intensity in the running segment is not high. We now evaluate the impact of λ on ρ_* in case (C), i.e., ρ_c . Figure 9 shows the results for $D(\rho)$ of approximate and exact analysis in case (C) when varying λ . From the figure, we can see that ρ_* increased subject to λ . The figure also shows that the approximate values for ρ_* again fitted well to those from the exact analysis. Recall here that λ is the key parameter for determining the optimal ρ (see Section V). As a result, the results in Figures 8 and 9 show that we can determine the optimal broadcast rate for all the vehicles in S_Q by only observing the traffic intensity λ .

C. Vehicles at Other Locations

We next consider the case where a transmitter is at other locations, i.e., not at the intersection, at the end of the queue, or the middle of the queue. Since our approximation assumes that N is sufficiently large and does not consider the distance from the end of the queue, we cannot obtain closed-form formulae for $p(r)$ or $\bar{M}(\rho)$ in general cases. However, vehicles at other locations can be considered as being in an intermediate state between the vehicle at the intersection and that at the end of the queue. Thus, it is expected that we can roughly estimate their performance by interpolating or extrapolating the values of approximate formulae for cases (A)–(C).

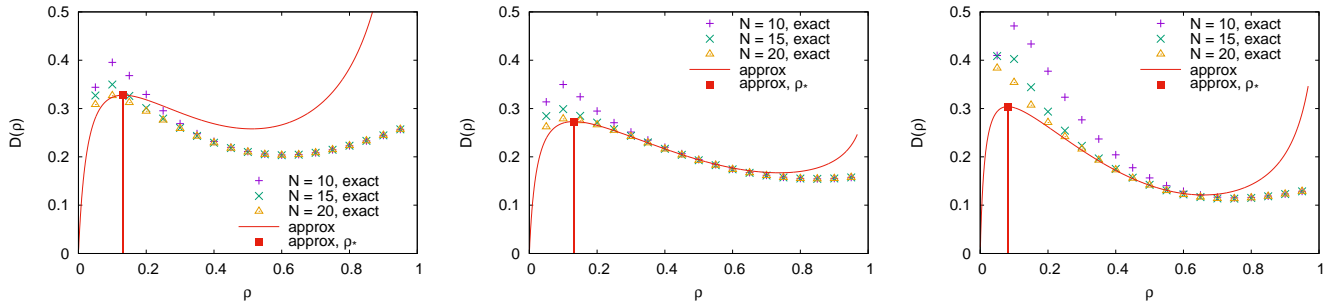


Fig. 7. Comparison of values of $D(\rho)$ from exact/approximate analysis with different ρ and N . Left, middle, and right graphs correspond to cases (A), (B), and (C). Vertical line represents ρ_* that maximizes approximate $D(\rho)$.

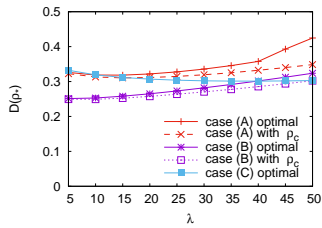


Fig. 8. Comparison of approximate $D(\rho_*)$ in cases (A)–(C) with different λ (solid line). Dashed and dotted lines represent $D(\rho_c)$ in cases (A) and (B), where $\rho_c = \rho_*$ in case (C).

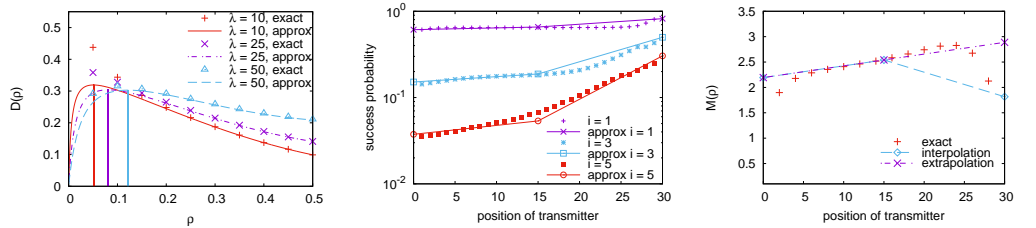


Fig. 9. Comparison of values of $D(\rho)$ from exact/approximate analysis with different ρ and λ in case (C). Vertical line represents ρ_* that maximizes approximate $D(\rho)$.

Figure 10 shows the values of $p(il_v)$ when varying the positions of the transmitter d and the distance to the receiver i in S_Q . We fixed $N = 30$ and $\rho = 0.1$, and the y -axis was in log scale. In the graph, the dashed lines represent the interpolation line using the approximation formulae for cases (A)–(C), where cases (A), (B), and (C) correspond to $d = 0$, $d = N/2 = 15$, and $d = 30$, respectively. In other words, the dashed line shows the *log-linear interpolation*. From the figure, we can see that the interpolation can give a rough estimation for the values of $p(il_v)$ in all cases. We can also see that if i increased, the results from the exact analysis become close to log-linear, whereas they tended to be a constant value when i was small. This is because if the receiver is closer to the transmitter, i.e., i is smaller, the impacts of the intersection or the end of the queue rapidly disappear as the distance from the transmitter to them increases. Similarly, Figure 11 shows the results for $\overline{M}(\rho)$, i.e., the mean number of successful receivers in S_Q when varying the positions of the transmitter d . Note that the y -axis is in linear scale. The dashed line was plotted by interpolating the results of the approximation for the three cases. The broken line was plotted by extrapolating the approximation for cases (A) and (C). We can see that if the positions of the transmitter were close to the middle of the queue, i.e., $N/2$, the extrapolation became a good estimation for the exact values. However, if the transmitter was close to the intersection or the end of the queue, the error increased. This tendency is similar to that in Figure 10. As a result, we can conclude the following. If the transmitter is close to the middle of the queue, we can use extrapolation on the basis of the approximate formulae for cases (A) and (C); otherwise, the approximate formulae for cases (A) and (B) should be used

Fig. 10. Comparison of $p(il_v)$ when varying position of transmitter at d -th vehicle from intersection. $N = 30$ and $\rho = 0.1$. Dashed line was plotted by interpolating the approximate formulae for cases (A) $d = 0$, (B) $d = 30$, and (C) $d = 15$.

instead.

VII. CONCLUSION

In this paper, we conducted a theoretical performance evaluation of vehicle-to-vehicle (V2V) broadcast communications at an intersection. We first derived the theoretical values of the probability of successful transmission and the mean number of successful receivers. We then provided a closed-form approximation for them. By using the approximation formulae, we provided a method for optimizing the broadcast rate of vehicles in the queueing segment. By using the closed-form formulae, we can obtain the optimal broadcast rate in a reasonable time without time-consuming numerical computation, which is required in exact analysis.

To maintain mathematical tractability, we assumed a simple channel model and media access control (MAC) layer in this paper, e.g., Rayleigh fading assumption or ALOHA. Thus, the generalization of the distribution of vehicles and fading are for future work. In addition, power control can be a good solution for the interference problem at an intersection. Therefore, the joint modeling and optimization of the broadcast rate and the transmission power of vehicles are also for future work. In addition, in our optimization method, we assume that the traffic intensities in running segments are given. However, vehicles/road side units need to infer these values in a practical situation, e.g., by measuring the distance to the vehicle running at the front. Such inference schemes and their impacts on our optimization method are also for future work.

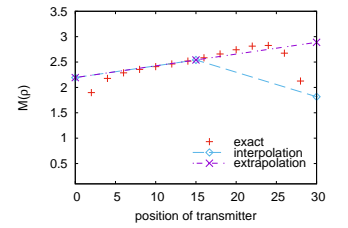


Fig. 11. Comparison of $\overline{M}(\rho)$ when varying position of transmitter from intersection. $N = 30$ and $\rho = 0.1$. Dashed line was plotted by interpolating approximation for cases (A) $d = 0$, (B) $d = 30$, and (C) $d = 15$. Broken line was plotted by extrapolating those for cases (A) and (C).

APPENDIX A APPROXIMATION METHODOLOGY

In this appendix, we give detailed explanations for the derivation of the approximate formulae presented in Section IV. For later use, we first introduce approximate formulae for $q_{n_0,T}(r | n_1)$ defined as

$$q_{n_0,T}(r | n_1) = \sum_{m=1}^{n_1} \log \left(1 + T \left(\frac{r}{n_0 + m} \right)^\alpha \right), \quad (29)$$

which plays an important role in our approximation method for $\mathcal{L}_{I_Q}(\mu T r^\alpha)$. Derivation of the following formulae with several auxiliary results are given in Appendix B.

Approximate formulae of $q_{n_0,T}(r | n_1)$: $q_{n_0,T}(r | n_1)$ can be approximated as follows.

(i) If $r < T^{-\frac{1}{\alpha}}(n_0 + 1)$,

$$q_{n_0,T}(r | n_1) \approx \begin{cases} \zeta(\alpha) T r^\alpha, & n_0 = 0, \\ \frac{T}{\alpha-1} \left[\frac{1}{n_0^{\alpha-1}} - \frac{1}{(n_0+n_1)^{\alpha-1}} \right] r^\alpha, & n_0 > 0, \end{cases}$$

where $\zeta(\alpha)$ ($\alpha > 0$) denotes the Riemann zeta function defined as

$$\zeta(\alpha) = \sum_{k=1}^{\infty} \frac{1}{k^\alpha}. \quad (30)$$

(ii) If $T^{-\frac{1}{\alpha}}(n_0 + 1) \leq r < T^{-\frac{1}{\alpha}}(n_0 + n_1)$,

$$\begin{aligned} q_{n_0,T}(r | n_1) &\approx (\alpha + \kappa_{1,\alpha} - \kappa_{2,\alpha}) T^{\frac{1}{\alpha}} r \\ &- \alpha \left(n_0 + \frac{1}{2} \right) \log T^{\frac{1}{\alpha}} r - \frac{T r^\alpha}{(\alpha-1)(n_0+n_1)^{\alpha-1}} \\ &- \frac{1}{2} \log \left(1 + T \left(\frac{r}{n_0+n_1} \right)^\alpha \right) - \psi_{n_0,T}(r) \\ &- \frac{1}{2} \log \left(1 + \frac{1}{T} \left(\frac{n_0}{r} \right)^\alpha \right) + \kappa_{1,\alpha} \\ &+ \alpha \log \frac{n_0!}{\sqrt{2\pi}} + \log 2, \end{aligned} \quad (31)$$

where

$$\psi_{n_0,T}(r) = n_0 \sum_{k=1}^{\infty} \frac{(-1)^{k+1}}{k(\alpha k + 1) T^k} \left(\frac{n_0}{r} \right)^{\alpha k}. \quad (32)$$

(iii) If $T^{-\frac{1}{\alpha}}(n_0 + n_1) \leq r$,

$$\begin{aligned} q_{n_0,T}(r | n_1) &\approx \alpha n_1 \log T^{\frac{1}{\alpha}} r \\ &+ \frac{1}{T} \left[\frac{n_0 + n_1}{\alpha + 1} + \frac{1}{2} \right] \left(\frac{n_0 + n_1}{r} \right)^\alpha \\ &- \frac{1}{T} \left[\frac{n_0}{\alpha + 1} + \frac{1}{2} \right] \left(\frac{n_0}{r} \right)^\alpha \\ &- \alpha \left(n_1 + n_0 + \frac{1}{2} \right) \log(n_0 + n_1) \\ &+ \alpha(n_0 + n_1) + \alpha \log \frac{n_0!}{\sqrt{2\pi}}. \end{aligned} \quad (33)$$

A. Derivation of Equations (7)–(12)

We first prove that (7) is true. To do this, we temporarily assume that $n_+ = n_- = N$. This assumption will be removed later by considering a sufficiently large N . Substituting $s = \mu T r^\alpha$ into (2) and letting $r = i l_v$ leads to

$$\begin{aligned} \mathcal{L}_{I_Q}(\mu T (i l_v)^\alpha) &= \prod_{m=-n_1, m \neq i, 0}^{n_+} \left[\frac{|i - m|^\alpha \rho}{|i - m|^\alpha + T i^\alpha} + 1 - \rho \right] \\ &= \frac{1 + T}{1 + (1 - \rho)T} \prod_{m=1, m \neq i}^{2N} \frac{1 + (1 - \rho)T \left| \frac{i}{i-m} \right|^\alpha}{1 + T \left| \frac{i}{i-m} \right|^\alpha} \\ &= \frac{1 + T}{1 + (1 - \rho)T} \prod_{m=1}^{N-i} \frac{1 + (1 - \rho)T \left(\frac{i}{m} \right)^\alpha}{1 + T \left(\frac{i}{m} \right)^\alpha} \\ &\times \prod_{m=1}^{N+i} \frac{1 + (1 - \rho)T \left(\frac{i}{m} \right)^\alpha}{1 + T \left(\frac{i}{m} \right)^\alpha}. \end{aligned} \quad (34)$$

It follows from (29) and (34) that

$$\begin{aligned} \log \mathcal{L}_{I_Q}(\mu T (i l_v)^\alpha) &= q_{0,(1-\rho)T}(i | N+i) + q_{0,(1-\rho)T}(i | N-i) \\ &- q_{0,T}(i | N+i) - q_{0,T}(i | N-i). \end{aligned} \quad (35)$$

We now assume that N is sufficiently large. Recall here that $(1 - \rho)T \geq 1$ and thus $((1 - \rho)T)^{-\frac{1}{\alpha}} < 1$. Therefore, we can apply (31) and thus obtain

$$q_{0,(1-\rho)T}(i | \infty) - q_{0,T}(i | \infty) \approx \xi_{\alpha,T}(\rho) i - \frac{1}{2} \log(1 - \rho), \quad (36)$$

where $\xi_{\alpha,T}(\rho)$ is defined in (8). It then follows from (35) that

$$\log \mathcal{L}_{I_Q}(\mu T (i l_v)^\alpha) \approx \log \frac{1 + T}{(1 - \rho)(1 + (1 - \rho)T)} + 2\xi_{\alpha,T}(\rho) i. \quad (37)$$

In addition, substituting $d = i l_v$ and $r = i l_v$ into (3) leads to

$$\begin{aligned} \log \mathcal{L}_{I_R^X}(\mu T (i l_v)^\alpha) &= -2\rho \lambda_x \int_0^\infty \frac{1}{(x/T^{\frac{1}{\alpha}} i l_v)^\alpha + 1} dx \\ &= -\rho \lambda_x C_{\alpha,T}^X i l_v. \end{aligned} \quad (38)$$

where $C_{\alpha,T}^X$ is given in (10). Similarly, from (4), we obtain

$$\begin{aligned} \log \mathcal{L}_{I_R^Y}(\mu T (i l_v)^\alpha | i l_v) &= -2\rho_0 \lambda_y \int_0^\infty \frac{T}{((y/i l_v)^2 + 1)^{\frac{\alpha}{2}} + T} dy \\ &= -\pi \rho_0 \lambda_y C_{\alpha,T}^Y i l_v. \end{aligned} \quad (39)$$

where $C_{\alpha,T}^Y$ is given in (10). As a result, combining (37)–(39) with (5) yields (7).

We now move on to the derivation of (11). For simplicity, we assume that $r = r_0 l_v$ ($r_0 \in \mathbb{N}$). This assumption will be removed later by extending the result to an arbitrary $r \in \mathbb{R}$.

By following the same arguments in the derivation of (34) and (35), we have

$$\begin{aligned} \log \mathcal{L}_{I_Q}(\mu Tr^\alpha) &= \sum_{\substack{m=-n_1 \\ m \neq 0}}^{n_+} \log \left[\frac{|r_0 - m|^\alpha \rho}{|r_0 - m|^\alpha + Ti^\alpha} + 1 - \rho \right] \\ &= \log(1 - \rho) + \log \frac{1 + T}{1 + (1 - \rho)T} + q_{0,(1-\rho)T}(r_0 | N + r_0) \\ &\quad + q_{0,(1-\rho)T}(r_0 | N - r_0) - q_{0,T}(r_0 | N + r_0) \\ &\quad - q_{0,T}(r_0 | N - r_0). \end{aligned}$$

Thus, similar to (36) and (37), letting $N \rightarrow \infty$ and $r_0 = r/l_v \in \mathbb{R}$ and applying (31) leads to

$$\log \mathcal{L}_{I_Q}(\mu Tr^\alpha) \approx 2\xi_{\alpha,T}(\rho) \frac{r}{l_v} + \log \frac{1 + T}{1 + (1 - \rho)T}.$$

From this, (5), (38), and (39), we obtain (11).

Finally, we derive (12). Since the receiver is in S_{R_y} at distance r from the intersection, its Euclidean distance from the i -th vehicle from the intersection is equal to $\sqrt{r^2 + (il_v)^2}$. However, applying this Euclidean distance to $\mathcal{L}_{I_Q}(\mu Tr^\alpha)$ leads to mathematically intractable analysis. Thus, we approximate this by using Manhattan distance, which is equal to $r + il_v$. Similar to in the previous case, we assume that $r = r_0 l_v$ ($r_0 \in \mathbb{N}$). It then follows from (2) that

$$\begin{aligned} \mathcal{L}_{I_Q}(\mu Tr^\alpha) &\approx \prod_{m=1}^{n_-} \frac{1 + (1 - \rho)T \left(\frac{r_0}{r_0+m} \right)^\alpha}{1 + T \left(\frac{r_0}{r_0+m} \right)^\alpha} \\ &\quad \times \prod_{m=1}^{n_+} \frac{1 + (1 - \rho)T \left(\frac{r_0}{r_0+m} \right)^\alpha}{1 + T \left(\frac{r_0}{r_0+m} \right)^\alpha}. \end{aligned} \quad (40)$$

By considering sufficiently large n_+ and n_- , we obtain

$$\log \mathcal{L}_{I_Q}(\mu Tr^\alpha) = 2(q_{r_0,(1-\rho)T}(r_0 | \infty) - q_{r_0,T}(r_0 | \infty)).$$

Since $((1 - \rho)T)^{-\frac{1}{\alpha}} < 1$, we can apply (31) to this and thus obtain

$$\begin{aligned} \log \mathcal{L}_{I_Q}(\mu Tr^\alpha) &\approx 2\xi_{\alpha,T}(\rho)r_0 - \left(r_0 + \frac{1}{2} \right) \log(1 - \rho) \\ &\quad - \log \frac{1 + \frac{1}{(1-\rho)T}}{1 + \frac{1}{T}} - 2(\underline{\psi}_{r_0,(1-\rho)T}(r_0) - \underline{\psi}_{r_0,T}(r_0)) \\ &\approx 2 \left[\xi_{\alpha,T}(\rho) - \log(1 - \rho) - \frac{\rho}{(\alpha + 1)(1 - \rho)T} \right] r_0 \\ &\quad - \log(1 - \rho) + \log \frac{(1 - \rho)(1 + T)}{1 + (1 - \rho)T}, \end{aligned} \quad (41)$$

where we use the following approximation [see (32)]

$$\begin{aligned} \underline{\psi}_{r_0,(1-\rho)T}(r_0) - \underline{\psi}_{r_0,T}(r_0) &= r_0 \sum_{k=1}^{\infty} \frac{(-1)^{k+1}}{k(\alpha k + 1)T^k} \\ &= \frac{r_0}{(\alpha + 1)T} \frac{\rho}{1 - \rho} + O(((1 - \rho)T)^2). \end{aligned} \quad (42)$$

Although the receiver is on the y -axis, $p(r)$ can be calculated very similarly to Proposition III.1. Indeed, we obtain

$$p(r) = \mathcal{L}_{I_Q}(\mu Tr^\alpha) \mathcal{L}_{I_R^X}(\mu Tr^\alpha) \mathcal{L}_{I_R^Y}(\mu Tr^\alpha | 0).$$

As a result, substituting (38)–(41) into the above yields (12). \square

B. Derivation of Equations (17)–(20)

We begin with (17). Similar to (34), we assume that $n_+ = n_- = N$ and consider a sufficiently large N . By substituting $s = \mu Tr^\alpha$ into (2) and letting $r = il_v$, we obtain

$$\begin{aligned} \mathcal{L}_{I_Q}(\mu T(il_v)^\alpha) &= \prod_{m=1}^{i-1} \frac{1 + (1 - \rho)T \left(\frac{i}{m} \right)^\alpha}{1 + T \left(\frac{i}{m} \right)^\alpha} \prod_{m=1}^{2N-i} \frac{1 + (1 - \rho)T \left(\frac{i}{m} \right)^\alpha}{1 + T \left(\frac{i}{m} \right)^\alpha} \\ &= \frac{1 + T}{1 + (1 - \rho)T} \prod_{m=1}^i \frac{1 + (1 - \rho)T \left(\frac{i}{m} \right)^\alpha}{1 + T \left(\frac{i}{m} \right)^\alpha} \\ &\quad \times \prod_{m=1}^{2N-i} \frac{1 + (1 - \rho)T \left(\frac{i}{m} \right)^\alpha}{1 + T \left(\frac{i}{m} \right)^\alpha}. \end{aligned}$$

By Using (29), the above equation can be rewritten as follows.

$$\begin{aligned} \log \mathcal{L}_{I_Q}(\mu Tr^\alpha) &= \log \frac{1 + T}{1 + (1 - \rho)T} + q_{0,(1-\rho)T}(i | i) \\ &\quad + q_{0,(1-\rho)T}(i | 2N - i) - q_{0,T}(i | i) - q_{0,T}(i | 2N - i). \end{aligned} \quad (43)$$

Since $((1 - \rho)T)^{-\frac{1}{\alpha}} < 1$, we can apply (33) and thus obtain

$$\begin{aligned} q_{0,(1-\rho)T}(i | i) - q_{0,T}(i | i) \\ \approx \left[\log(1 - \rho) + \frac{\rho}{T(1 - \rho)(\alpha + 1)} \right] i + \frac{\rho}{2T(1 - \rho)}. \end{aligned} \quad (44)$$

Note that if we assume that N is sufficiently large, we can use the approximation in (36). As a result, substituting this and (44) into (43) and combining it with (38) and (16) lead to (17) and (18).

We now prove that (19) is true. Similar to the derivation of (11) and (12), suppose that $r = r_0 l_v$ ($r_0 \in \mathbb{N}$). Note here that if the r_0 -th vehicle in S_Q from the transmitter is currently transmitting, the transmission to the receiver fails. Therefore, from (2), (29) and (43), we obtain

$$\begin{aligned} \log \mathcal{L}_{I_Q}(\mu Tr^\alpha) &= \log(1 - \rho) + \log \frac{1 + T}{1 + (1 - \rho)T} \\ &\quad + q_{0,(1-\rho)T}(r_0 | r_0) + q_{0,(1-\rho)T}(r_0 | 2N - r_0) \\ &\quad - q_{0,T}(r_0 | r_0) - q_{0,T}(r_0 | 2N - r_0). \end{aligned}$$

Plugging (44) into the above and combining it with (38) and (16) yields (19).

Finally, we consider (20). In this case, if we assume that $r = r_0 l_v$, (2) leads to

$$\mathcal{L}_{I_Q}(\mu Tr^\alpha) = \prod_{m=1}^{n_-+n_+} \frac{1 + (1 - \rho)T \left(\frac{r_0}{r_0+m} \right)^\alpha}{1 + T \left(\frac{r_0}{r_0+m} \right)^\alpha}.$$

Therefore, by following the same arguments in the derivation of (12) and (41), we can readily show that (20) holds. \square

APPENDIX B AUXILIARY RESULTS

In this appendix, we discuss the approximation method for $q_{n_0,T}(r | n_1)$ defined in (29). We first provide several lemmas, which are required for the approximation. All proofs of the lemmas are given in Appendix C. Using these results, we derive approximate formulae of $q_{n_0,T}(r | n_1)$.

To begin with, we define $\eta_{r,T}$ such that

$$\eta_{r,T} = \min \left\{ m \in \mathbb{N}; \left(\frac{r}{n_0 + m} \right)^\alpha < \frac{1}{T} \right\} - 1. \quad (45)$$

In accordance with the value of $\eta_{r,T}$, we can consider three subcases: (i) $\eta_{r,T} = 0$; (ii) $1 \leq \eta_{r,T} \leq n_1$; and (iii) $n_1 < \eta_{r,T}$. In what follows, we provide lemmas corresponding to each subcase. Note that we only use the results corresponding to cases (ii) and (iii) in the main part of our paper, but, we also consider case (i) $\eta_{r,T} = 0$ for completeness in this appendix.

We start with case (i) $\eta_{r,T} = 0$. By definition, this case suggests that

$$T \left(\frac{r}{n_0 + 1} \right)^\alpha < 1. \quad (46)$$

We then have the following lemma, which provides an estimation of $q_{n_0,T}(r | n_1)$ under the condition in which (46) holds.

Lemma B.1 Suppose that $\eta_{r,T} = 0$, i.e., (46) holds. If $n_0 = 0$, then

$$q_{0,T}(r | n_1) = \zeta(\alpha) Tr^\alpha + O((Tr^\alpha)^2) + O(Tr^\alpha n_1^{-\alpha+1}), \quad (47)$$

otherwise, if $n_0 \geq 1$, then

$$\begin{aligned} q_{n_0,T}(r | n_1) &= T \left[\frac{n_0}{\alpha - 1} + \frac{1}{2} \right] \left(\frac{r}{n_0} \right)^\alpha \\ &- T \left[\frac{(n_0 + n_1)}{\alpha - 1} + \frac{1}{2} \right] \left(\frac{r}{n_0 + n_1} \right)^\alpha \\ &+ O(Tr^\alpha n_0^{-\alpha-1}) + O(Tr^\alpha (n_0 + n_1)^{-\alpha-1}) \\ &+ O((Tr^\alpha)^2 n_0^{1-2\alpha}) + O((Tr^\alpha)^2 (n_0 + n_1)^{1-2\alpha}). \end{aligned} \quad (48)$$

We next consider case (ii) $1 \leq \eta_{r,T} \leq n_1$, i.e.,

$$\left(1 + \frac{1}{n_0 + \eta_{r,T}} \right)^{-\alpha} \leq T \left(\frac{r}{n_0 + \eta_{r,T} + 1} \right)^\alpha < 1. \quad (49)$$

To proceed, we divide $q_{n_0,T}(r | n_1)$ into the following partial-sums:

$$\begin{aligned} \bar{q}_{n_0,T}(r | n_1) &= \sum_{m=\eta_{r,T}+1}^{n_1} \log \left(1 + T \left(\frac{r}{n_0 + m} \right)^\alpha \right), \\ \underline{q}_{n_0,T}(r) &= \sum_{m=1}^{\eta_{r,T}} \log \left(1 + T \left(\frac{r}{n_0 + m} \right)^\alpha \right). \end{aligned} \quad (50)$$

Lemma B.2 below shows upper and lower bounds for $\bar{q}_{n_0,T}(r | n_1)$.

Lemma B.2 If $\eta_{r,T}$ given in (45) satisfies $1 \leq \eta_{r,T} \leq n_1$, there exist $\bar{q}_{\text{lwr}}(\eta_{r,T} | n_1)$ and $\bar{q}_{\text{upr}}(\eta_{r,T} | n_1)$ such that

$$\bar{q}_{\text{lwr}}(\eta_{r,T} | n_1) < \bar{q}_{n_0,T}(r | n_1) \leq \bar{q}_{\text{upr}}(\eta_{r,T} | n_1), \quad (51)$$

and

$$\begin{aligned} \bar{q}_{\text{upr}}(\eta_{r,T} | n_1) &= (\kappa_{1,\alpha} - \log 2) (n_0 + \eta_{r,T} + 1) - \bar{\psi}_{n_0,n_1,T}(r) \\ &- \frac{1}{2} \log \left(1 + T \left(\frac{r}{n_0 + n_1} \right)^\alpha \right) + \frac{1}{2} \log 2 \\ &+ O((n_0 + \eta_{r,T})^{-1}) + O((n_0 + n_1)^{-1}), \end{aligned} \quad (52)$$

and

$$\begin{aligned} \bar{q}_{\text{lwr}}(\eta_{r,T} | n_1) &= \bar{\varphi}(\eta_{r,T}) (n_0 + \eta_{r,T} + 1) - \bar{\psi}_{n_0,n_1,T}(r) \\ &- \frac{1}{2} \log \left(1 + T \left(\frac{r}{n_0 + n_1} \right)^\alpha \right) \\ &+ \frac{1}{2} \log \left(1 + \left(1 + \frac{1}{n_0 + \eta_{r,T}} \right)^{-\alpha} \right) \\ &+ O((n_0 + \eta_{r,T})^{-1}) + O((n_0 + n_1)^{-1}), \end{aligned} \quad (53)$$

where $\kappa_{1,\alpha}$ is given in (9) and

$$\bar{\varphi}(\eta_{r,T}) = \sum_{k=1}^{\infty} \frac{(-1)^{k+1}}{k(\alpha k - 1)} \left(1 + \frac{1}{n_0 + \eta_{r,T}} \right)^{-\alpha k}, \quad (54)$$

$$\bar{\psi}_{n_0,n_1,T}(r) = (n_0 + n_1) \sum_{k=1}^{\infty} \frac{(-1)^{k+1} T^k}{k(\alpha k - 1)} \left(\frac{r}{n_0 + n_1} \right)^{\alpha k}. \quad (55)$$

We next give upper and lower bounds for $\underline{q}_{n_0,T}(r)$.

Lemma B.3 If $\eta_{r,T}$ given in (45) satisfies $1 \leq \eta_{r,T} \leq n_1$ and $\alpha \in \mathbb{N}$, then there exist $\underline{q}_{\text{upr}}(\eta_{r,T})$ and $\underline{q}_{\text{lwr}}(\eta_{r,T})$ such that

$$\underline{q}_{\text{lwr}}(\eta_{r,T}) < \underline{q}_{n_0,T}(r) < \underline{q}_{\text{upr}}(\eta_{r,T}), \quad (56)$$

and

$$\begin{aligned} \underline{q}_{\text{upr}}(\eta_{r,T}) &= (\alpha + \log 2 - \kappa_{2,\alpha}) (n_0 + \eta_{r,T}) - \underline{\psi}_{n_0,T}(r) \\ &- \frac{1}{2} \log \left(1 + \frac{1}{T} \left(\frac{n_0}{r} \right)^\alpha \right) + \alpha \log \left(1 + \frac{1}{n_0 + \eta_{r,T}} \right) \eta_{r,T} \\ &- \alpha \left(n_0 + \frac{1}{2} \right) \log(n_0 + \eta_{r,T}) + \alpha \log \frac{n_0!}{\sqrt{2\pi}} \\ &+ \frac{1}{2} \log 2 + O \left((n_0 + \eta_{r,T})^{-1} \frac{1}{T} \left(\frac{n_0 + \eta_{r,T}}{r} \right)^\alpha \right), \end{aligned} \quad (57)$$

and

$$\begin{aligned} \underline{q}_{\text{lwr}}(\eta_{r,T}) &= (\alpha + \underline{\varphi}(\eta_{r,T})) (n_0 + \eta_{r,T}) - \underline{\psi}_{n_0,T}(r) \\ &- \frac{1}{2} \log \left(1 + \frac{1}{T} \left(\frac{n_0}{r} \right)^\alpha \right) - \alpha \left(n_0 + \frac{1}{2} \right) \log(n_0 + \eta_{r,T}) \\ &+ \alpha \log \frac{n_0!}{\sqrt{2\pi}} + \frac{1}{2} \log \left(1 + \left(1 + \frac{1}{n_0 + \eta_{r,T}} \right)^{-\alpha} \right) \\ &+ O \left((n_0 + \eta_{r,T})^{-1} \frac{1}{T} \left(\frac{n_0 + \eta_{r,T}}{r} \right)^\alpha \right), \end{aligned} \quad (58)$$

where $\kappa_{2,\alpha}$ and $\underline{\psi}_{n_0,T}(r)$ are given in (9) and (32), respectively and

$$\underline{\varphi}(\eta_{r,T}) = \sum_{k=1}^{\infty} \frac{(-1)^{k+1}}{k(\alpha k + 1)} \left(1 + \frac{1}{n_0 + \eta_{r,T}} \right)^{-\alpha k}, \quad (59)$$

Finally, we consider case (iii), i.e., the following holds, for any $m \in [1, n_1]$,

$$T \left(\frac{r}{n_0 + m} \right)^\alpha \geq T \left(\frac{r}{n_0 + n_1} \right)^\alpha > 1. \quad (60)$$

Lemma B.4 If $\eta_{r,T}$ given in (45) satisfies $n_1 \leq \eta_{r,T}$ and $\alpha \in \mathbb{N}$, then

$$\begin{aligned} q_{n_0,T}(r | n_1) &= \alpha n_1 \log T^{\frac{1}{\alpha}} r + \alpha(n_0 + n_1) + \alpha \log \frac{n_0!}{\sqrt{2\pi}} \\ &\quad - \alpha \left(n_0 + n_1 + \frac{1}{2} \right) \log(n_0 + n_1) \\ &\quad + \frac{1}{T} \left[\frac{n_0 + n_1}{\alpha + 1} + \frac{1}{2} \right] \left(\frac{n_0 + n_1}{r} \right)^\alpha \\ &\quad - \frac{1}{T} \left[\frac{n_0}{\alpha + 1} + \frac{1}{2} \right] \left(\frac{n_0}{r} \right)^\alpha \\ &\quad + O \left((n_0 + n_1)^{-1} \frac{1}{T} \left(\frac{n_0 + n_1}{r} \right)^\alpha \right) \\ &\quad + O \left(\frac{1}{T^2} \left(\frac{n_0}{r} \right)^{2\alpha} \right) + O \left(\log \left(1 + \frac{1}{n_0 + n_1} \right) \right). \end{aligned} \quad (61)$$

We next derive approximate formulae for $q_{n_0,T}(r | n_0)$ on the basis of Lemmas B.1–B.4. In cases (i) and (iii) where $\eta_{r,T} = 0$ and $\eta_{r,T} \geq n_1$, approximate formulae are directly obtained by applying Lemmas B.1 and B.4. Therefore, we only consider case (ii) $1 \leq \eta_{r,T} < n_1$ in what follows and explain how we derive the approximate formulae from Lemmas B.2 and B.3.

Note first that

$$\log \left(1 + \left(1 + \frac{1}{n_0 + \eta_{r,T}} \right)^{-\alpha} \right) \approx \log 2, \quad (62)$$

for sufficiently large $n_0 + \eta_{r,T}$. Therefore, (9) and (54) suggest that

$$\begin{aligned} \bar{\varphi}(\eta_{r,T}) &= \sum_{k=1}^{\infty} (-1)^{k+1} \left[\frac{\alpha}{\alpha k - 1} - \frac{1}{k} \right] \left(1 + \frac{1}{n_0 + \eta_{r,T}} \right)^{-\alpha k} \\ &\approx \kappa_{1,\alpha} - \log 2, \end{aligned} \quad (63)$$

for sufficiently large $n_0 + \eta_{r,T}$. In addition, $\psi_{n_0,n_1,T}(r)$ can be rewritten as [see (55)]

$$\begin{aligned} \bar{\psi}_{n_0,n_1,T}(r) &= \frac{(n_0 + n_1)T}{\alpha - 1} \left(\frac{r}{n_0 + n_1} \right)^\alpha \\ &\quad + O \left((n_0 + n_1)T^2 \left(\frac{r}{n_0 + n_1} \right)^{2\alpha} \right). \end{aligned}$$

Furthermore, from the definition [see (45)], $\eta_{r,T}$ can be approximated as

$$\eta_{r,T} \approx T^{1/\alpha} r - n_0. \quad (64)$$

Therefore, by combining these facts with (51)–(55), we can obtain the following approximation for $\bar{q}_{n_0,T}(r | n_1)$:

$$\begin{aligned} \bar{q}_{n_0,T}(r | n_1) &\approx (\kappa_{1,\alpha} - \log 2) T^{\frac{1}{\alpha}} r + \kappa_{1,\alpha} + \frac{1}{2} \log 2 \\ &\quad - \frac{Tr^\alpha}{(\alpha - 1)(n_0 + n_1)^{\alpha-1}} + \frac{1}{2} \log \left(1 + T \left(\frac{r}{n_0 + n_1} \right)^\alpha \right). \end{aligned} \quad (65)$$

Similar to the above arguments, it can be said that [see (9)]

$$\begin{aligned} \underline{\varphi}(\eta_{r,T}) &= \sum_{k=1}^{\infty} (-1)^{k+1} \left[\frac{1}{k} - \frac{\alpha}{\alpha k + 1} \right] \left(1 + \frac{1}{n_0 + \eta_{r,T}} \right)^{-\alpha k} \\ &\approx \log 2 - \kappa_{2,\alpha}, \end{aligned}$$

for sufficiently large $n_0 + \eta_{r,T}$. Applying this, (62) and (64) to (56)–(59), we can approximate $\underline{q}_{n_0,T}(r)$ as

$$\begin{aligned} \underline{q}_{n_0,T}(r) &\approx (\alpha + \log 2 - \kappa_{2,\alpha}) T^{\frac{1}{\alpha}} r - \underline{\psi}_{n_0,T}(r) \\ &\quad - \frac{1}{2} \log \left(1 + \frac{1}{T} \left(\frac{n_0}{r} \right)^\alpha \right) - \alpha \left(n_0 + \frac{1}{2} \right) \log T^{\frac{1}{\alpha}} r \\ &\quad + \alpha \log \frac{n_0!}{\sqrt{2\pi}} + \frac{1}{2} \log 2. \end{aligned} \quad (66)$$

As a result, by combining (65) and (66), we obtain (31).

APPENDIX C PROOFS

A. Proof of Lemma B.1

It follows from Taylor's theorem that

$$\log(1 + x^\alpha) = \sum_{k=1}^{\infty} \frac{(-1)^{k+1}}{k} (x^\alpha)^k, \quad x^\alpha < 1, \quad (67)$$

from which and (29) we obtain

$$\begin{aligned} q_{n_0,T}(r | n_1) &= \sum_{m=n_0+1}^{n_0+n_1} \sum_{k=1}^{\infty} \frac{(-1)^{k+1} T^k}{k} \left(\frac{r}{m} \right)^{\alpha k} \\ &= \sum_{k=1}^{\infty} \frac{(-1)^{k+1} T^k r^{\alpha k}}{k} \sum_{m=n_0+1}^{n_0+n_1} \left(\frac{1}{m} \right)^{\alpha k}. \end{aligned} \quad (68)$$

Furthermore, applying the Euler-Maclaurin summation formula to the Riemann zeta function leads to (see e.g., Section 6.4 in [30] for details)

$$\sum_{m=1}^n \frac{1}{m^\alpha} = \zeta(\alpha) + \frac{n^{1-\alpha}}{1-\alpha} - \frac{n^{-\alpha}}{2} + O(n^{-\alpha-1}), \quad (69)$$

where $\zeta(\alpha)$ is given in (30). Therefore, applying (69) to (68) and letting $n_0 = 0$ yields

$$q_{0,T}(r | n_1) = \sum_{k=1}^{\infty} \frac{(-1)^{k+1} (Tr^\alpha)^k}{k} [\zeta(\alpha k) + O(n_1^{1-\alpha k})],$$

from which, we obtain (47). On the other hand, if $n_0 \geq 1$, by using (69), the last summation in (68) can be rewritten as

$$\begin{aligned} \sum_{m=n_0+1}^{n_0+n_1} \left(\frac{1}{m} \right)^{\alpha k} &= \sum_{m=1}^{n_0+n_1} \left(\frac{1}{m} \right)^{\alpha k} - \sum_{m=1}^{n_0} \left(\frac{1}{m} \right)^{\alpha k} \\ &= \frac{n_0^{1-\alpha k} - (n_0 + n_1)^{1-\alpha k}}{\alpha k - 1} + \frac{n_0^{-\alpha k} - (n_0 + n_1)^{-\alpha k}}{2} \\ &\quad + O(n_0^{-\alpha k-1}) + O((n_0 + n_1)^{-\alpha k-1}). \end{aligned}$$

Thus, plugging the above into (68), we obtain

$$\begin{aligned} q_{n_0,T}(r | n_1) &= \sum_{k=1}^{\infty} \frac{(-1)^{k+1} (Tr^\alpha)^k}{k} \\ &\quad \times \left[\frac{n_0^{1-\alpha k} - (n_0 + n_1)^{1-\alpha k}}{\alpha k - 1} + \frac{n_0^{-\alpha k} - (n_0 + n_1)^{-\alpha k}}{2} \right. \\ &\quad \left. + O(n_0^{-\alpha k-1}) + O((n_0 + n_1)^{-\alpha k-1}) \right], \end{aligned}$$

which leads to (48).

B. Proof of Lemma B.2

Note first that $T(\frac{r}{m})^\alpha < 1$ for any $m > n_0 + \eta_{r,T}$ according to the definition of $\eta_{r,T}$ [see (49)]. Thus, similar to the derivation of (68), we obtain

$$\bar{q}_{n_0,T}(r | n_1) = \sum_{k=1}^{\infty} \frac{(-1)^{k+1} T^k r^{\alpha k}}{k} \sum_{m=n_0+\eta_{r,T}+1}^{n_0+n_1} \left(\frac{1}{m}\right)^{\alpha k}. \quad (70)$$

Furthermore, it follows from (69) that, for any $k \in \mathbb{N}$,

$$\begin{aligned} \sum_{m=n_0+\eta_{r,T}+1}^{n_0+n_1} \left(\frac{1}{m}\right)^{\alpha k} &= \sum_{m=1}^{n_0+n_1} \left(\frac{1}{m}\right)^{\alpha k} - \sum_{m=1}^{n_0+\eta_{r,T}} \left(\frac{1}{m}\right)^{\alpha k} \\ &= \frac{(n_0 + \eta_{r,T} + 1)^{1-\alpha k}}{\alpha k - 1} - \frac{(n_0 + n_1)^{1-\alpha k}}{\alpha k - 1} \\ &\quad + \frac{(n_0 + \eta_{r,T} + 1)^{-\alpha k}}{2} - \frac{(n_0 + n_1)^{-\alpha k}}{2} \\ &\quad + O((n_0 + \eta_{r,T} + 1)^{-\alpha k-1}) + O((n_0 + n_1)^{-\alpha k-1}). \end{aligned} \quad (71)$$

Thus, applying (67) and (71) to (70) leads to

$$\begin{aligned} \bar{q}_{n_0,T}(r | n_1) &= \sum_{k=1}^{\infty} \frac{(-1)^{k+1}}{k} \\ &\quad \times \left[\left(\frac{n_0 + \eta_{r,T} + 1}{\alpha k - 1} + \frac{1}{2} \right) T^k \left(\frac{r}{n_0 + \eta_{r,T} + 1} \right)^{\alpha k} \right. \\ &\quad - \left(\frac{n_0 + n_1}{\alpha k - 1} + \frac{1}{2} \right) T^k \left(\frac{r}{n_0 + n_1} \right)^{\alpha k} \\ &\quad + O \left((n_0 + \eta_{r,T} + 1)^{-1} T^k \left(\frac{r}{n_0 + \eta_{r,T} + 1} \right)^{\alpha k} \right) \\ &\quad \left. + O \left((n_0 + n_1)^{-1} T^k \left(\frac{r}{n_0 + n_1} \right)^{\alpha k} \right) \right]. \end{aligned} \quad (72)$$

In addition, (49) suggests that

$$\begin{aligned} \sum_{k=1}^{\infty} \frac{(-1)^{k+1} T^k}{k} \left(\frac{n_0 + \eta_{r,T} + 1}{\alpha k - 1} + \frac{1}{2} \right) \left(\frac{r}{n_0 + \eta_{r,T} + 1} \right)^{\alpha k} \\ &< \sum_{k=1}^{\infty} \frac{(-1)^{k+1} T^k}{k} \left[\frac{n_0 + \eta_{r,T} + 1}{\alpha k - 1} + \frac{1}{2} \right] \\ &= \sum_{k=1}^{\infty} \frac{(-1)^{k+1}}{k(\alpha k - 1)} (n_0 + \eta_{r,T} + 1) + \frac{1}{2} \log 2 \\ &= \sum_{k=1}^{\infty} (-1)^{k+1} \left[\frac{\alpha}{\alpha k - 1} - \frac{1}{k} \right] (n_0 + \eta_{r,T} + 1) + \frac{1}{2} \log 2 \\ &= (\kappa_{1,\alpha} - \log 2)(n_0 + \eta_{r,T} + 1) + \frac{1}{2} \log 2, \end{aligned} \quad (73)$$

where we use $\sum_{k=1}^{\infty} (-1)^{k+1}/k = \log 2$ in the first and last equalities and $\kappa_{1,\alpha}$ is given in (9). Furthermore, using (67), we obtain

$$\begin{aligned} \sum_{k=1}^{\infty} \frac{(-1)^{k+1} T^k}{k} \left(\frac{r}{n_0 + n_1} \right)^{\alpha k} \\ = \log \left(1 + T \left(\frac{r}{n_0 + n_1} \right)^{\alpha} \right). \end{aligned} \quad (74)$$

Therefore, combining (55), (73), and (74) with (72), the second inequality in (51) and (52), i.e., the upper bound for $\bar{q}_{n_0,T}(r | n_1)$, is proved.

We next prove the first inequality in (51), i.e., the lower bound. Similar to the derivation of (73), combining (49) with (71) yields

$$\begin{aligned} \sum_{k=1}^{\infty} \frac{(-1)^{k+1} T^k}{k} \left(\frac{n_0 + \eta_{r,T} + 1}{\alpha k - 1} + \frac{1}{2} \right) \left(\frac{r}{n_0 + \eta_{r,T} + 1} \right)^{\alpha k} \\ \geq \sum_{k=1}^{\infty} \frac{(-1)^{k+1}}{k} \left(\frac{n_0 + \eta_{r,T} + 1}{\alpha k - 1} + \frac{1}{2} \right) \left(1 + \frac{1}{n_0 + \eta_{r,T}} \right)^{-\alpha k} \\ = \varphi(\eta_{r,T}) (n_0 + \eta_{r,T} + 1) \\ + \frac{1}{2} \log \left(1 + \left(1 + \frac{1}{n_0 + \eta_{r,T}} \right)^{-\alpha} \right), \end{aligned}$$

where we use (54) and (67) in the equality. Consequently, substituting this, (55), and (74) into (72) leads to (51) and (53).

C. Proof of Lemma B.3

From Taylor's theorem, we obtain for $x > 1$,

$$\log(1+x^\alpha) = \log x^\alpha + \sum_{k=1}^{\infty} \frac{(-1)^{k+1}}{k} \frac{1}{x^{\alpha k}}.$$

Since $T(\frac{r}{n_0+m})^\alpha > 1$ for any $m \in [1, \eta_{r,T}]$, applying the above equation to (50) leads to

$$\begin{aligned} &\bar{q}_{n_0,T}(r) \\ &= \sum_{m=n_0+1}^{n_0+\eta_{r,T}} \log T \left(\frac{r}{m} \right)^\alpha + \sum_{m=n_0+1}^{n_0+\eta_{r,T}} \sum_{k=1}^{\infty} \frac{(-1)^{k+1}}{k T^k} \left(\frac{m}{r} \right)^{\alpha k} \\ &= \eta_{r,T} \log T + \alpha (\eta_{r,T} \log r - \log(n_0 + \eta_{r,T})_{\eta_{r,T}}) \\ &\quad + \sum_{k=1}^{\infty} \frac{(-1)^{k+1}}{k T^k} \left(\frac{1}{r} \right)^{\alpha k} \sum_{m=1}^{\eta_{r,T}} (n_0 + m)^{\alpha k}, \end{aligned} \quad (75)$$

where $(x)_k$ ($k \in \mathbb{N}$) denotes the falling sequential product such that

$$(x)_k = x(x-1) \cdots (x-k+1).$$

It follows from Faulhaber's formula (see e.g., [31]) that for any $n \in \mathbb{N}$,

$$\begin{aligned} &\sum_{m=1}^n (n_0 + m)^{\alpha k} \\ &= \frac{1}{\alpha k + 1} \sum_{j=0}^{\alpha k} \binom{\alpha k + 1}{j} B_j [(n_0 + n)^{\alpha k + 1 - j} - (n_0)^{\alpha k + 1 - j}] \\ &= \frac{1}{\alpha k + 1} \sum_{j=0}^{\alpha k} \binom{\alpha k + 1}{j} B_j \\ &\quad \times (n_0 + n)^{\alpha k + 1 - j} \left[1 - \left(\frac{n_0}{n_0 + n} \right)^{\alpha k + 1 - j} \right], \end{aligned} \quad (76)$$

where B_j 's are the Bernoulli numbers such that

$$B_0 = 1, \quad B_j = \sum_{k=0}^{j-1} (-1)^k \binom{j+1}{k} B_k, \quad j \geq 1.$$

Substituting (76) into the second term on the right-hand side of (75) yields

$$\begin{aligned}
& \sum_{k=1}^{\infty} \frac{(-1)^{k+1}}{kT^k} \left(\frac{1}{r} \right)^{\alpha k} \sum_{m=1}^{\eta_{r,T}} (n_0 + m)^{\alpha k} \\
&= \sum_{k=1}^{\infty} \frac{(-1)^{k+1}}{kT^k} \left(\frac{1}{r} \right)^{\alpha k} \frac{1}{\alpha k + 1} \sum_{j=0}^{\alpha k} \binom{\alpha k + 1}{j} B_j \\
&\quad \times (n_0 + \eta_{r,T})^{\alpha k + 1 - j} \left[1 - \left(\frac{n_0}{n_0 + \eta_{r,T}} \right)^{\alpha k + 1 - j} \right] \\
&= \sum_{k=1}^{\infty} \frac{(-1)^{k+1}}{kT^k} \left[\left(\frac{n_0 + \eta_{r,T}}{\alpha k + 1} + \frac{1}{2} \right) \left(\frac{n_0 + \eta_{r,T}}{r} \right)^{\alpha k} \right. \\
&\quad \left. - \left(\frac{n_0}{\alpha k + 1} + \frac{1}{2} \right) \left(\frac{n_0}{r} \right)^{\alpha k} + \frac{r^{-\alpha k}}{\alpha k + 1} \sum_{j=2}^{\alpha k} \binom{\alpha k + 1}{j} B_j \right. \\
&\quad \left. \times (n_0 + \eta_{r,T})^{\alpha k + 1 - j} \left[1 - \left(\frac{n_0}{n_0 + \eta_{r,T}} \right)^{\alpha k + 1 - j} \right] \right]. \tag{77}
\end{aligned}$$

Note that (45) and $1 \leq \eta_{r,T}$ suggest that

$$\left(1 + \frac{1}{n_0 + \eta_{r,T}} \right)^{-\alpha} < \frac{1}{T} \left(\frac{n_0 + \eta_{r,T}}{r} \right)^{\alpha} \leq 1. \tag{78}$$

Note also that (see (32) and (67))

$$\begin{aligned}
& \sum_{k=1}^{\infty} \frac{(-1)^{k+1}}{kT^k} \left(\frac{n_0}{\alpha k + 1} + \frac{1}{2} \right) \left(\frac{n_0}{r} \right)^{\alpha k} \\
&= \underline{\psi}_{n_0, T}(r) + \frac{1}{2} \log \left(1 + \frac{1}{T} \left(\frac{n_0}{r} \right)^{\alpha} \right). \tag{79}
\end{aligned}$$

Thus, by using (78) and (79), we obtain

$$\begin{aligned}
& \sum_{k=1}^{\infty} \frac{(-1)^{k+1}}{kT^k} \left[\left(\frac{n_0 + \eta_{r,T}}{\alpha k + 1} + \frac{1}{2} \right) \left(\frac{n_0 + \eta_{r,T}}{r} \right)^{\alpha k} \right. \\
&\quad \left. - \left(\frac{n_0}{\alpha k + 1} + \frac{1}{2} \right) \left(\frac{n_0}{r} \right)^{\alpha k} \right] \\
&\leq \sum_{k=1}^{\infty} \frac{(-1)^{k+1}}{k} \left[\frac{n_0 + \eta_{r,T}}{\alpha k + 1} + \frac{1}{2} \right] - \underline{\psi}_{n_0, T}(r) \\
&\quad - \frac{1}{2} \log \left(1 + \frac{1}{T} \left(\frac{n_0}{r} \right)^{\alpha} \right) \\
&= (\log 2 - \kappa_{2,\alpha}) (n_0 + \eta_{r,T}) + \frac{1}{2} \log 2 - \underline{\psi}_{n_0, T}(r) \\
&\quad - \frac{1}{2} \log \left(1 + \frac{1}{T} \left(\frac{n_0}{r} \right)^{\alpha} \right), \tag{80}
\end{aligned}$$

where $\kappa_{2,\alpha}$ is given in (9) and we use $\sum_{k=1}^{\infty} (-1)^{k+1}/k = \log 2$ in the equality. Similarly, we have

$$\begin{aligned}
& \sum_{k=1}^{\infty} \frac{(-1)^{k+1}}{kT^k} \left[\left(\frac{n_0 + \eta_{r,T}}{\alpha k + 1} + \frac{1}{2} \right) \left(\frac{n_0 + \eta_{r,T}}{r} \right)^{\alpha k} \right. \\
&\quad \left. - \left(\frac{n_0}{\alpha k + 1} + \frac{1}{2} \right) \left(\frac{n_0}{r} \right)^{\alpha k} \right] \\
&\geq \sum_{k=1}^{\infty} \frac{(-1)^{k+1}}{k} \left[\frac{n_0 + \eta_{r,T}}{\alpha k + 1} + \frac{1}{2} \right] \left(1 + \frac{1}{n_0 + \eta_{r,T}} \right)^{-\alpha k} \\
&\quad - \underline{\psi}_{n_0, T}(r) - \frac{1}{2} \log \left(1 + \frac{1}{T} \left(\frac{n_0}{r} \right)^{\alpha} \right) \\
&= \underline{\varphi}(\eta_{r,T})(n_0 + \eta_{r,T}) + \frac{1}{2} \log \left(1 + \left(1 + \frac{1}{n_0 + \eta_{r,T}} \right)^{-\alpha} \right) \\
&\quad - \underline{\psi}_{n_0, T}(r) - \frac{1}{2} \log \left(1 + \frac{1}{T} \left(\frac{n_0}{r} \right)^{\alpha} \right), \tag{81}
\end{aligned}$$

where the equality follows from (59) and (79). Furthermore, it follows from (78) that

$$\begin{aligned}
& \sum_{k=1}^{\infty} \frac{(-1)^{k+1}}{T^k k (\alpha k + 1)} \sum_{j=2}^{\alpha k} \binom{\alpha k + 1}{j} B_j \\
&\quad \times \frac{(n_0 + \eta_{r,T})^{\alpha k + 1 - j}}{r^{\alpha k}} \left[1 - \left(\frac{n_0}{n_0 + \eta_{r,T}} \right)^{\alpha k + 1 - j} \right] \\
&= O \left((n_0 + \eta_{r,T})^{-1} \frac{1}{T} \left(\frac{n_0 + \eta_{r,T}}{r} \right)^{\alpha} \right). \tag{82}
\end{aligned}$$

Therefore, the lower and upper bounds for the last term on the right-hand side of (75) are shown.

We next consider the first and second terms in (75). It follows from Stirling's formula that

$$\begin{aligned}
& \eta_{r,T} \log r - \log(n_0 + \eta_{r,T})_{\eta_{r,T}} \\
&= \eta_{r,T} \log r - \log \sqrt{2\pi(n_0 + \eta_{r,T})} \\
&\quad - (n_0 + \eta_{r,T}) \log \left(\frac{n_0 + \eta_{r,T}}{e} \right) + \log n_0! \\
&\quad + O \left(\log \left(1 + \frac{1}{n_0 + \eta_{r,T}} \right) \right) \\
&= n_0 + \eta_{r,T} + \eta_{r,T} \log \left(\frac{r}{n_0 + \eta_{r,T}} \right) + \log \frac{n_0!}{\sqrt{2\pi}} \\
&\quad - \left(n_0 + \frac{1}{2} \right) \log(n_0 + \eta_{r,T}) + O \left(\log \left(1 + \frac{1}{n_0 + \eta_{r,T}} \right) \right). \tag{83}
\end{aligned}$$

Note that (78) suggests that

$$\log \left(\frac{r}{n_0 + \eta_{r,T}} \right) > \log \frac{1}{T^{1/\alpha}}, \tag{84}$$

$$\log \left(\frac{r}{n_0 + \eta_{r,T}} \right) \leq \log \frac{1}{T^{1/\alpha}} \left(1 + \frac{1}{n_0 + \eta_{r,T}} \right). \tag{85}$$

As a result, combining (85) with (83) and using this, (80), (82), and (77), we obtain (56) and (57). Similarly, by combining (84) with (83) and applying this, (81), and (82) into (77), we obtain (56) and (58).

D. Proof of Lemma B.4

Similar to the derivation of (75), it follows from (60) that

$$\begin{aligned}
& q_{n_0, T}(r) \\
&= \sum_{m=n_0+1}^{n_0+n_1} \log T \left(\frac{r}{m} \right)^\alpha + \sum_{m=n_0+1}^{n_0+n_1} \sum_{k=1}^{\infty} \frac{(-1)^{k+1}}{k T^k} \left(\frac{m}{r} \right)^{\alpha k} \\
&= n_1 \log T + \alpha (n_1 \log r - \log(n_0 + n_1)_{n_1}) \\
&\quad + \sum_{k=1}^{\infty} \frac{(-1)^{k+1}}{k T^k} \left(\frac{1}{r} \right)^{\alpha k} \sum_{m=1}^{n_1} (n_0 + m)^{\alpha k}. \tag{86}
\end{aligned}$$

Applying the same technique in the derivation of (77) to the second term in (86) yields

$$\begin{aligned}
& \sum_{k=1}^{\infty} \frac{(-1)^{k+1}}{k T^k} \left(\frac{1}{r} \right)^{\alpha k} \sum_{m=1}^{n_1} (n_0 + m)^{\alpha k} \\
&= \sum_{k=1}^{\infty} \frac{(-1)^{k+1}}{k T^k} \left[\left(\frac{n_0 + n_1}{\alpha k + 1} + \frac{1}{2} \right) \left(\frac{n_0 + n_1}{r} \right)^{\alpha k} \right. \\
&\quad \left. - \left(\frac{n_0}{\alpha k + 1} + \frac{1}{2} \right) \left(\frac{n_0}{r} \right)^{\alpha k} \right. \\
&\quad \left. + O(r^{-\alpha k} n_0^{\alpha k-1}) + O(r^{-\alpha k} (n_0 + n_1)^{\alpha k-1}) \right] \\
&= \frac{1}{T} \left[\frac{n_0 + n_1}{\alpha + 1} + \frac{1}{2} \right] \left(\frac{n_0 + n_1}{r} \right)^\alpha \\
&\quad - \frac{1}{T} \left[\frac{n_0}{\alpha + 1} + \frac{1}{2} \right] \left(\frac{n_0}{r} \right)^\alpha + O \left(\frac{1}{T} \frac{n_0^{\alpha-1}}{r^\alpha} \right) \\
&\quad + O \left((n_0 + n_1)^{-1} \frac{1}{T} \left(\frac{n_0 + n_1}{r} \right)^\alpha \right). \tag{87}
\end{aligned}$$

In addition, similar to (83), Stirling's formula leads to

$$\begin{aligned}
& n_1 \log r - \log(n_0 + n_1)_{n_1} \\
&= n_0 + n_1 + n_1 \log \left(\frac{r}{n_0 + n_1} \right) + \log \frac{n_0!}{\sqrt{2\pi}} \\
&\quad - \left(n_0 + \frac{1}{2} \right) \log(n_0 + n_1) + O \left(\log \left(1 + \frac{1}{n_0 + n_1} \right) \right).
\end{aligned}$$

Substituting this and (87) into (86) results in (61).

REFERENCES

- [1] H. Hartenstein and K. Laberteaux, *VANET Vehicular Applications and Inter-Networking Technologies*. New York: Wiley, 2009.
- [2] *Wireless Access in Vehicular Environment (WAVE) in Standard 802.11, Specific Requirements*, IEEE Std. 802.11p/D1.0, Feb. 2006.
- [3] *Wireless Access in Vehicular Environment: Networking Services*, IEEE Std. 1609.3, 2007.
- [4] Vehicle Safety Commun. Consortium (VSCC), Vehicle safety communications project, task 3 final report: Identify intelligent vehicle safety applications enabled by DSRC, Nat. Highway Traffic Safety Admin., Washington, DC, USA, 2005.
- [5] C.-L. Huang, Y. P. Fallah, R. Sengupta, and H. Krishnan, "Adaptive intervehicle communication control for cooperative safety systems," *IEEE Network*, vol. 24, no. 1, pp. 6–13, 2010.
- [6] Y. P. Fallah, C. Huang, R. Sengupta, and H. Krishnan, "Congestion control based on channel occupancy in vehicular broadcast networks," In *Proc. VTC-2010 Fall*, Sep. 2010, pp. 1–5.
- [7] Y. P. Fallah, N. Nasiriani, and H. Krishnan, "Stable and fair power control in vehicle safety networks," *IEEE Trans. on Veh. Technol.*, vol. 65, no. 3, pp. 1662–1675, 2016.
- [8] T. Tieler, D. Jiang, Q. Chen, L. Delgrossi, and H. Hartenstein, "Design methodology and evaluation of rate adaptation based congestion control for vehicle safety communications," In *Proc. VNC'11*, Nov. 2011, pp. 116–123.
- [9] M. Torrent-Moreno, J. Mittag, P. Santi, and H. Hartenstein, "Vehicle-to-vehicle communication: fair transmit power control for safety-critical information," *IEEE Trans. on Veh. Technol.*, vol. 58, no. 7, pp. 3684–3703, 2009.
- [10] J. Mittag, F. Schmidt-Eisenlohr, M. Killat, J. Härri, and H. Hartenstein, "Analysis and design of effective and low-overhead transmission power control for VANETs," In *Proc. VANET*, 2008, pp. 39–48.
- [11] T. Kimura and H. Saito, "Theoretical interference analysis of inter-vehicular communication at intersection with power control," In *Proc. ACM MSWiM '16*, Nov. 2016, pp. 3–10.
- [12] M. Torrent-Moreno, J. Mittag, P. Santi, and H. Hartenstein, "Broadcast reception rates and effects of priority access in 802.11-based vehicular ad-hoc networks," In *Proc. VANET*, 2004, pp. 10–18.
- [13] S. Eichler, "Performance evaluation of the IEEE 802.11p WAVE communication standard," In *Proc. VTC-2007 Fall*, Oct. 2007, pp. 2199–2203.
- [14] J. C. Burguillo-Rial, E. Costa-Montenegro, F. Gil-Castineira, and P. Rodriguez-Hernandez, "Performance analysis of IEEE 802.11p in urban environments using a multi-agent model," In *Proc. PIMRC*, Sep. 2008, pp. 1–6.
- [15] Y. P. Fallah, C. L. Huan, R. Sengupta, and H. Krishnan, "Analysis of information dissemination in vehicular ad-hoc networks with application to cooperative vehicle safety systems," *IEEE Trans. on Veh. Technol.*, vol. 60, no. 1, pp. 233–247, 2011.
- [16] A. T. Gian and A. Busson, "Modeling CSMA/CA in VANET," *Analytical and Stochastic Modeling Techniques and Applications, Lecture Notes in Computer Science* vol. 7314, pp. 91–105, 2012.
- [17] C. Han, M. Dianati, R. Tafazoli, R. Kernchen, and X. Shen, "Analytical study of the IEEE 802.11p MAC sublayer in vehicular networks," *IEEE Trans. on Intell. Transp. Syst.*, vol. 13, no. 2, pp. 873–886, 2012.
- [18] Y. Yao, L. Rao and X. Liu, "Performance and reliability analysis of IEEE 802.11p safety communication in a highway environment," *IEEE Trans. on Veh. Technol.*, vol. 62, no. 9, pp. 4198–4212, 2013.
- [19] D. Stoyan, W. S. Kendall, and J. Mecke, *Stochastic Geometry and its Applications*. Second Edition, Chichester: John Wiley & Sons, 1995.
- [20] M. Haenggi, J. G. Andrews, F. Baccelli, O. Dousse, and M. Franceschetti, "Stochastic geometry and random graphs for the analysis and design of wireless networks," *IEEE J. Sel. A. Commun.*, vol. 27, no. 7, pp. 1029–1046, 2009.
- [21] J. G. Andrews, F. Baccelli, and R. K. Ganti, "A tractable approach to coverage and rate in cellular networks," *IEEE Trans. on Commun.*, vol. 59, no. 11, pp. 3122–3134, 2011.
- [22] B. Błaszczyzyn, P. Muhlethaler, and Y. Toor, "Stochastic analysis of Aloha in vehicular ad-hoc networks," *Ann. Telecommun.*, vol. 68, no. 1, pp. 95–106, 2012.
- [23] M. J. Farooq, H. ElSawy, and M.-S. Alouini, "Modeling inter-vehicle communication in multi-lane highways: a stochastic geometry approach," In *Proc. VTC-2015 Fall*, Sep. 2015, pp. 1–5.
- [24] T. V. Nguyen, F. Baccelli, K. Zhu, S. Subramanian, and W. Wu, "A performance analysis of CSMA based broadcast protocol in VANETs," In *Proc. INFOCOM'13*, Apr. 2013, pp. 14–19.
- [25] Z. Tong, H. Lu, M. Haenggi, and C. Poellabauer, "A stochastic geometry approach to the modeling of DSRC for vehicular safety communication," *IEEE Trans. on Intell. Transp. Syst.*, vol. 17, no. 5, pp. 1448–1458, 2016.
- [26] T. V. Nguyen, F. Baccelli, and D. Kofman, "A stochastic geometry analysis of dense IEEE 802.11 networks," In *Proc. INFOCOM'07*, May 2007, pp. 1199–1207.
- [27] G. Karagiannis, O. Altintas, E. Ekici, G. Heijenk, B. Jarupan, K. Lin, and T. Wei, "Vehicular networking: a survey and tutorial on requirements, architectures, challenges, standards and solutions," *IEEE Commun. Surveys Tuts.*, vol. 13, no. 4, pp. 584–616, 2011.
- [28] H. ElSawy and E. Hossain, "A modified hard core point process for analysis of random CSMA wireless networks in general fading environments," *IEEE Trans. Commun.*, vol. 61, no. 4, pp. 1520–1534, 2013.
- [29] F. Baccelli and B. Błaszczyzyn, *Stochastic Geometry and Wireless Networks, Volume I -Theory*. Hanover: Now Publishers, 2009.
- [30] H. M. Edwards, *Riemann's Zeta Function*. Paperback edition, Mineola: Dover Publications, 2001.
- [31] J. H. Conway and R. Guy, *The Book of Numbers*. Second edition, New York: Springer, 1996.